

Article

# Groundwater Characterization by Means of Conservative ( $\delta^{18}\text{O}$ and $\delta^2\text{H}$ ) and Non-Conservative ( $^{87}\text{Sr}/^{86}\text{Sr}$ ) Isotopic Values: The Classical Karst Region Aquifer Case (Italy–Slovenia)

Chiara Calligaris <sup>1,\*</sup> , Kim Mezga <sup>2</sup>, Francesca Federica Slejko <sup>1</sup>, Janko Urbanc <sup>3</sup> and Luca Zini <sup>1</sup> 

<sup>1</sup> Mathematics and Geosciences Department (DMG), University of Trieste, Via Weiss, 23, 4128 Trieste, Italy; fslejko@units.it (F.F.S.); zini@units.it (L.Z.)

<sup>2</sup> Slovenian National Building and Civil Engineering Institute, Dimičeva ulica, 12, 1000 Ljubljana, Slovenia; kim.mezga@zag.si

<sup>3</sup> Geological Survey of Slovenia, Dimičeva ulica, 14, 1000 Ljubljana, Slovenia; janko.urbanc@geo-zs.si

\* Correspondence: calligar@units.it; Tel.: +39-040-558-2019

Received: 31 July 2018; Accepted: 21 August 2018; Published: 28 August 2018



**Abstract:** The study of the different hydrogeological compartments is a prerequisite for understanding and monitoring different fluxes, thereby evaluating the environmental changes in an ecosystem where anthropogenic disturbances are present in order to preserve the most vulnerable groundwaters from contamination and degradation. In many karst domains in the Mediterranean, areas groundwaters and surface waters are a single system, as a result of the features that facilitate the ingress of waters from surface to subsurface. This is also the case for the Classical Karst hydrostructure, which is a carbonate plateau that rises above the northern Adriatic Sea, shared between Italy and Slovenia. The main suppliers to the aquifer are the effective precipitations and the waters from three different rivers: Reka/Timavo, Soča/Isonzo and Vipava/Vipacco. Past and ongoing hydrogeological studies on the area have focused on the connections within the Classical Karst Region aquifer system through the analysis of water caves and springs hydrographs and chemographs. In this paper, the authors present new combined data from major ions, oxygen, hydrogen and strontium stable and radiogenic isotopes which have allowed a more complementary knowledge of the groundwater circulation, provenance and water-rock interactions. All the actions occurred in the framework of the European project HYDROKARST.

**Keywords:** Classical Karst Region; groundwater; geochemistry; oxygen ( $\delta^{18}\text{O}$ ) and hydrogen ( $\delta^2\text{H}$ ) stable isotopes; radiogenic  $^{87}\text{Sr}/^{86}\text{Sr}$  isotopic ratio; water management; caves; HYDROKARST project

## 1. Introduction

Karst aquifers host large reservoirs of groundwater, and reconciling environmental protection of water bodies with human requirements, requests an accurate and up to date assessment of the available resources and their vulnerability. This is particularly important for the European Union, where carbonate aquifers supply approximately 75% to 80% of drinking and agricultural waters [1]. Often, classical hydrogeological studies are not enough to shed light on the groundwater hydrodynamics of karst environments, due to the complex flow paths in fracture and karst conduits systems [2]. For this reason, the use of different approaches and techniques facilitate to understand the complex karst hydrodynamics that can be significantly improved, using combined geochemical and oxygen, hydrogen and strontium (O, H and Sr) isotope systematics [2–6]. Groundwater geochemistry

provides the means to better define the aquifer systems, their water sources, the geochemical evolution as a result of water-rock interaction and gives a unique insight into its dynamics. Naturally occurring isotopes, such as oxygen and hydrogen isotopic composition ( $\delta^{18}\text{O}$  and  $\delta^2\text{H}$ ), are used as tracers to comprehend water dynamics, e.g., groundwater recharge areas, its source and movement [7,8]. Unlike stable isotopes of oxygen and hydrogen, which have long been used in karst hydrogeology, strontium isotopes do not fractionate in nature in carbonate rocks. Hence, the strontium isotope ratios ( $^{87}\text{Sr}/^{86}\text{Sr}$ ) give precious insight into water-rock interaction processes [2,9–17] which depend on velocity, infiltration flux, aquifer thickness and weathering rates [9].

In the Classical Karst Region, the use of Sr isotopic ratio has been firstly applied within the European project named HYDROKARST, i.e., *Karst aquifer as a strategic cross-border water resource*, with the aim of joined protection and management of shared transboundary Classical Karst Region groundwater system.

The area is a cross-border karst plateau, shared between the north-eastern part of Italy and western Slovenia, particularly interesting from a hydrogeological point of view, it has been studied for more than 200 years, pushed by the necessity of providing fresh drinking waters for the increasing Italian and Slovenian population.

Past hydrogeological studies focused on the hydrodynamics trying to define the connections between Reka River and the underground karst system [18–30].

Only in the 1980s begun the studies that were based on stable isotopes which suggested that the Soča/Isonzo River has a widespread influence on the Classical Karst aquifer [6,31–39].

The current knowledge and new cross-border projects as agreements enabled the selection of joint monitoring sites of the shared aquifer, which contributed to a deeper understand of the dynamics of the system, as well as on the chemical and isotopic composition of groundwaters. The goals of the present study are: to characterize the hydrogeochemical components of the Classical Karst Region groundwater system and to show the effectiveness of combining geochemical analyses to strontium isotope systematic.

## 2. The Study Area: Geological, Structural, Geomorphological and Hydrogeological Setting

The Classical Karst Region is a limestone plateau of 750 km<sup>2</sup> which rises above the Adriatic Sea (Figure 1). It extends NW-SE 50 km long from the Soča/Isonzo River (Italy) to Brkini Hills near Škocjan (Slovenia). It is 15–20 km wide, gentle dipping toward NW, from 450 m a.s.l. in Škocjan (Slovenia) to the Sea level (Timavo Springs in Italy).

The plateau is an anticlinorium (the “Trieste-Komen anticlinorium” of [40]) consisting of platform limestones and dolomites (Lower Cretaceous to Upper Paleocene) bounded to the East, North and South by the Upper Eocene marls and sandstones of a siliciclastic turbidite, the Flysch Formation [41–43]. Along its western edge the plateau is overlain by the relatively permeable Quaternary alluvial deposits of the Friuli plain [44–47].

Although the vertical and lateral lithofacies variations are frequent, the carbonate succession is predominantly calcareous and is therefore the site of a well karstified aquifer. The dolomitic and dolomitic calcareous layers, which sometimes act as aquitards, are more frequent at the bottom of the succession, and hence can be identified in correspondence of the anticlinorium's core, outcropping in the middle of the plateau.

From the structural point of view, two have been the main tectonic phases which impacted on the investigated area: the mesoalpine or dinaric which had a prevailing NE-SW compression trend, and the neoalpine one with a compressive trend NNE-SSW to N-S oriented. The main evidences are the thrusts identifiable along the cliffs facing the northern Adriatic Sea as the “Thrust del Carso”, the Divača and Raša faults [43,45,47] (Figure 1). The compressions squeezed the thick carbonate succession, giving rise to a wide anticline fold which in turn overlapped and locally overthrust the turbiditic succession. The asymmetric anticline is not continuous, it is segmented by smaller faults result of the neoalpine compressions.

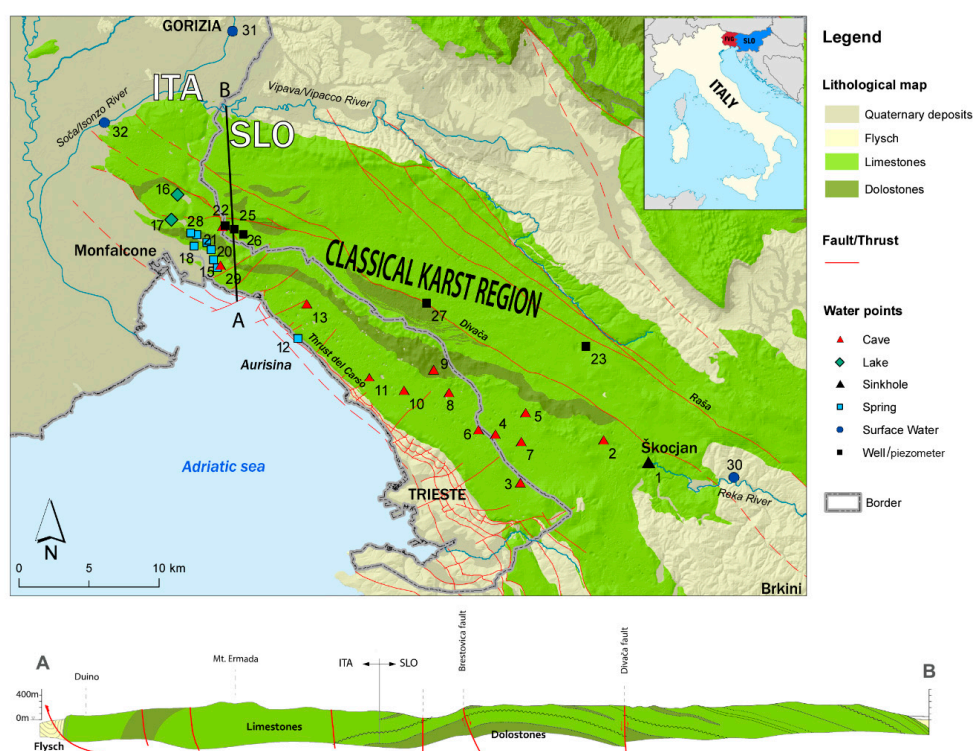


**Figure 1.** Study area overview, lithological map and simplified cross-section (A–B). The numbers close to the symbols represent the points of the karst hydrostructure where the waters can be identified: Škocjanske jame (1); Kačna jama (2); Grotta Skilan (3); Brezno v Stržinkni dolini (4); Jama v Kanjaduach (5); Abisso di Trebiciano (6); B3G—Brezno treh generacij (7); Grotta meravigliosa di Lazzaro Jerko (8); Abisso di Rupingrande (9); Grotta Gigante (10); Abisso Massimo (11); Aurisina spring (12); Grotta Lindner (13); Timavo Spring (14); Sardos Spring (15); Doberdò Lake (16); Pietrarossa Lake (17); Lisert springs (18); Moschenizze North Spring (19); Moschenizze South Spring (20); Sablici 4 Spring (21); B4 – Klariči pumping station (22); Štorje piezometer (23); Cavernetta di Comarie (24); B2 piezometer (25); B9 piezometer (26); P1 piezometer (27); Sablici 16 Spring (28); Pozzo dei colombi (29); Reka River (30); Soča/Isonzo River Is1 (31); Soča/Isonzo River Is2 (32).

The analyses conducted by Cucchi and Zini [38] recognize in the structures one of the main controlling factor in the evolution of the karst features: a trend in the discontinuities controlled by the Alpine and Dinaric stresses gave rise to a network of fractures from which the main conduit and doline's alignments formed. The maximum dip of the strata and the main sub-vertical discontinuities represent in fact, the preferential directions for conduits and shafts development.

The long lasting exposure of the plateau shaped it into a mature karst. Even if in the Italian Friuli Venezia Giulia Region and in Slovenia, the Classical Karst Region is one of the several renewed karst areas [48–52], it is the most famous karst area in the world where the word *karst* was used for the first time [53,54]. It is known worldwide for the high density and variety of caves and surface karst morphotypes [49]: in the limited area of the Italian Karst (about 200 km<sup>2</sup>) there are more than 3500 known caves (of which more than 150 develop for more than hundred meters; a dozen develops for a thousand meters). Eighty sinkholes, more than 100 m wide, and limestone pavements with a total surface area of several square kilometres are present. On the Slovenia side, the known caves are about 1000 [45] and surely the Škocjanske jame caves (included in the UNESCO's (United Nations Educational, Scientific and Cultural Organization) World Heritage List since 1986) are among the most interesting and known show caves in the world.

From a speleogenetical viewpoint, the plateau emerged at least ten million years ago, during one of the paroxysmal phases of the alpine-dinaric orogeny. The genesis of the karst faced with

different phases. According to the nature of voids, the water was primarily stored and transmitted through the matrix. During the Messinian crisis, the circulating groundwaters enlarged the fissures developing defined pathways as pipes (conduits or caves). The network consists in shallow paths running in the hypogean part between Škocjanske jame and Trebiciano Abyss. In the last kilometres before outflowing, the waters, even if channelized in wide conduits, rise up from considerable depths (as witnessed by the cave diver explorations, which reached depths of more than 80 m b.s.l., [29]) in correspondence of the Timavo Springs.

The Classical Karst Region groundwaters are at times identifiable as a result of the caves present in the area, witnesses of the highly karstified environment and real “windows” in the hydrostructure, allowing the study of the otherwise inaccessible and untouchable waters. Waters of the Reka/Timavo River were identified at the locations B3G Brezno treh generacij (SLO) (Figure 1(No.7)), Kačna Jama (SLO) (Figure 1(No.2)), Jama v Kanjaducah (SLO) (Figure 1(No.5)), Brezno v Stršinkni dolini (SLO) (Figure 1(No.4)), Abisso di Trebiciano (ITA) (Figure 1(No.6)) and Pozzo dei Colombi (ITA) (Figure 1(No.29)) [45]. Only during flood periods or heavy rainstorms the groundwaters of the Classical Karst Region aquifer reach the Abisso Massimo (Figure 1(No.11)), Abisso di Rupingrande (Figure 1(No.9)), Grotta Skilan (Figure 1(No.3)), Grotta Lindner (Figure 1(No.13)), Grotta meravigliosa di Lazzaro Jerko (Figure 1(No.8)) and Grotta Gigante (Figure 1(No.10)) caves (all ITA) [45,55].

The aquifer’s recharge is due to three different contributions: (1) the autogenic recharge which derives from the precipitations on the karst area, (2) the allogenic recharge which is due to the contribution of the Reka River, and (3) the influent character of the Soča/Isonzo and Vipava/Vipacco rivers (Figure 1).

- (1) The effective infiltrations (*karst waters*) contribute to the recharge with 20.6 m<sup>3</sup>/s [24].
- (2) The Soča/Isonzo springs originate under the glaciated mountains of the Julian Alps in Slovenia. The waters cross the Italian border after 96 km and flow into the Adriatic Sea. It is the second largest river of the Friuli Venezia Giulia Region. Its average discharge, 5 km inland from the Adriatic Sea, is 134 m<sup>3</sup>/s [56]. The porous aquifer of the Isonzo/Soča and Vipacco/Vipava alluvial plain provides a further substantial but more diffuse recharge estimated in 10 m<sup>3</sup>/s [26,29,36,37,44,57–60].
- (3) The Reka River flows on the surface for approximately half part of its course on flysch lithologies (31 km calculated on a hypothetical straight path), from Snežnik Mountain (Slovenian-Croatian border area) to the larger swallow hole of Škocjanske jame. Its mean discharge is evaluated in 8.26 m<sup>3</sup>/s and the discharge range from 0.18 m<sup>3</sup>/s to 305 m<sup>3</sup>/s according to the Environmental Agency of the Republic of Slovenia [61].

The main outflows of the aquifer are located NW of the plateau, along its SW-facing edge. In this area, the more productive springs are tapped either for actual water supply (Sardos, Figure 1(No.15)) or for reserve purposes (Timavo, Moschenizze North, Figure 1(No.19)). About 2 km North of these springs the Klariči pumping wells (Figure 1(No.22)) extract a mean rate of 100 L/s [39].

Several are the minor outflows fenced in a few square kilometres along the coast belt from Aurisina to Monfalcone town. The main outflow is the Timavo Spring (Figure 1(No.14), mean discharge of 29.3 m<sup>3</sup>/s), at the second place there is Sardos (Figure 1(No.15), mean discharge of 1.9 m<sup>3</sup>/s), and in third place all the other smaller springs as Aurisina (Figure 1(No.12), mean discharge of 0.3 m<sup>3</sup>/s), Moschenizze South (Figure 1(No.20), mean discharge of 0.1 m<sup>3</sup>/s), Pietrarossa (Figure 1(No.17)) and Sablici (Figure 1(No.21), mean discharge of 1.2 m<sup>3</sup>/s), Moschenizze North (Figure 1(No.19)) and Lisert (Figure 1(No.18), mean discharge of 1.8 m<sup>3</sup>/s) [29,58,59,62]. To these outflows, it is important to add the contribution of the submerged costal springs arising below the sea level that have a mean estimated discharge of 0.5–1 m<sup>3</sup>/s [58].

### 3. Materials and Methods: Sampling and Analytical Procedures

The three-year (2012–2014) project took the realization of several monitoring surveys during which selected springs, surface- and ground-water points were sampled (Figure 2).

During the project lifetime, a total of 125 water samples were collected and analyzed within 5 different field sampling surveys. Sampling periods were chosen accordingly to the hydrogeological conditions evaluating the water discharge at the Timavo Spring. The first survey was held on 11–12 September 2012 with a discharge of 12 to 10 m<sup>3</sup>/s at the Timavo springs and of 0.5 m<sup>3</sup>/s at the Reka River (low flow conditions) where the last flood higher than 10 m<sup>3</sup>/s was recorded in the beginning of May. The second survey was realized in wintertime, on 14 January 2013 with a measured discharge of 28 m<sup>3</sup>/s (average flow conditions) at the Timavo springs and a discharge of 2.5 m<sup>3</sup>/s at the Reka River. The third one was done on 8–10 April 2013. The discharge conditions were decreasing with values of 89–83 m<sup>3</sup>/s (recorded at the Timavo springs) and of 17–27 m<sup>3</sup>/s at the Reka River where in the previous days two important floods with more than 90 m<sup>3</sup>/s of discharged water occurred. The fourth sampling survey was done on 29–31 July 2013 in low flow conditions; the measured discharge was 13 m<sup>3</sup>/s at Timavo springs and 0.7 m<sup>3</sup>/s at the Reka River (point 30, Figure 1), one and a half months after the last flood. The last, fifth, sampling survey was done on 31 March and 1 April 2014 with discharge of 39 m<sup>3</sup>/s at Timavo Spring and a discharge of 4.5 m<sup>3</sup>/s at the Reka River, where a peak discharge of 15.8 m<sup>3</sup>/s occurred one week before the survey.

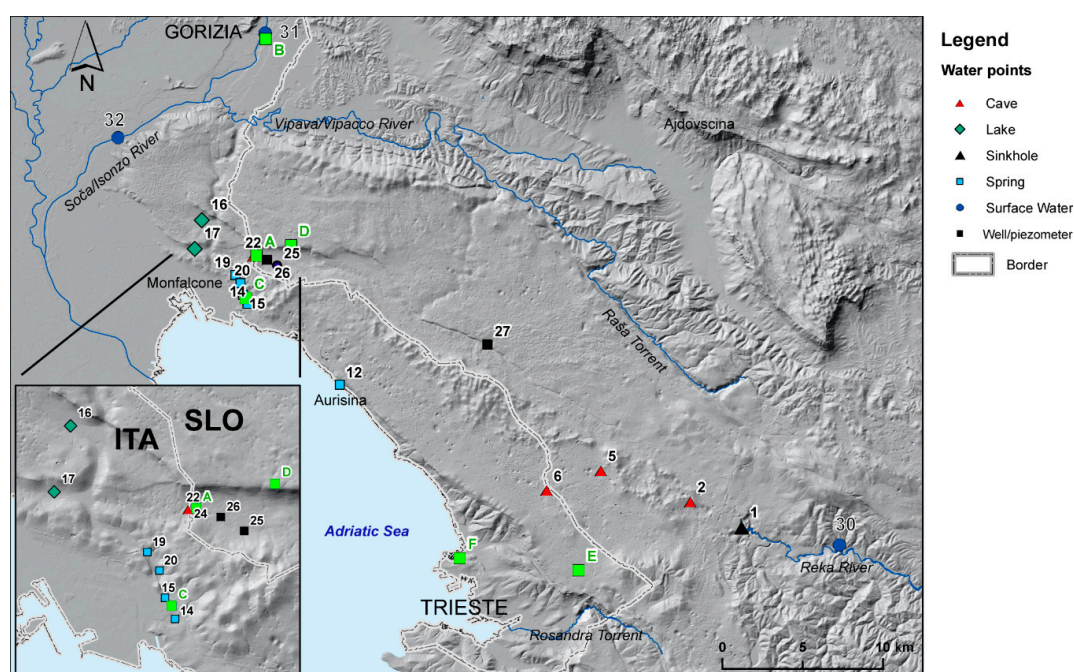


**Figure 2.** Sampling points within the study area. In the box (left below) the zoom is highlighting the spring area at San Giovanni di Duino. Green squares represent the pluviometers: A—Klariči; B—Gorizia; C—Randaccio; D—Sela na Krasu; E—Brestovizza; F—Filzi-Trieste. The other points are: Škocjanske jame (1); Kačna jama (2); Jama v Kanjaducah (5); Abisso di Trebiciano (6); Aurisina spring (12); Timavo Spring (14); Sardos Spring (15); Doberdò Lake (16); Pietrarossa Lake (17); Moschenitze North Spring (19); Moschenitze South Spring (20); B4—Klariči pumping station (22); Štorje piezometer (23); Cavernetta di Comarie (24); B2 piezometer (25); B9 piezometer (26); P1 piezometer (27); Reka River (30); Soča/Isonzo River Is1 (31); Soča/Isonzo River Is2 (32).

Temperature (T), pH, Electrical Conductivity (EC), major elements (anions and cations) and silica (SiO<sub>2</sub>) (Table 1) as well as the environmental isotopes ( $\delta^{18}\text{O}$ ,  $\delta^2\text{H}$ ,  $^{87}\text{Sr}/^{86}\text{Sr}$ ) were determined (Table 2). The T, pH and EC of each water sample were measured in situ using a conductivity meter WTW Cond 330i standardised to 25 °C and a pH meter (Hanna HI 991300), respectively. Each water sample was sealed in a pre-cleaned polyethylene bottle. For major ion analyses 1 L of water was sampled at each location, for stable isotopes  $\delta^{18}\text{O}$  and  $\delta^2\text{H}$  0.1 L and for strontium isotopes ( $^{87}\text{Sr}/^{86}\text{Sr}$ ) 0.25 L.

Water samples were chemically analyzed by the AcegasApsAmga (Trieste, Italy) laboratory which for major ions used the ion chromatography (940 Professional IC Vario by Metrohm with the IC-NET software (Baxter Medication Delivery Products, Riverview, FL, USA)) according to the procedures defined for the waters intended for human consumption by the Italian Law 31/2001 with a precision less than  $\leq 10\%$  and a detection limit of 0.1 mg/L for anions  $\text{Cl}^-$ ,  $\text{SO}_4^{2-}$ ,  $\text{PO}_4^{2-}$  and  $\text{NO}_3^-$ . For cations  $\text{Na}^+$ ,  $\text{K}^+$ ,  $\text{Mg}^{2+}$  and  $\text{Ca}^{2+}$  the detection limit was of 0.5 mg/L. Bicarbonates ( $\text{HCO}_3^-$ ) were analyzed using the Titrimetry with a sensitivity of 1 mg/L (Table 1). Before any consideration regarding water characterisation the ion balance check was done.

Analyses of the stable isotopes of  $\delta^{18}\text{O}$  and  $\delta^2\text{H}$  were carried out at Hydroisotop GmbH laboratory (Schweitenkirchen, Germany) on a laser-based cavity ring down spectrometer (CRDS, Picarro L-2130i with autosampler (PICARRO, INC. Santa Clara, CA, USA) [63]). The CRDS analyses the isotopic composition of water vapour by measuring the isotopologue-specific laser absorption values. Every sample was proceeded and measured six times, from which the last four analyses were used to determine the isotopic composition of the sample by average. Analytical errors of the method are  $\pm 0.10\text{‰}$  for  $\delta^{18}\text{O}$  and  $\pm 1.0\text{‰}$ , for  $\delta^2\text{H}$ , respectively. Values for deuterium excess ( $d$ -excess;  $d = \delta^2\text{H} - 8 \cdot \delta^{18}\text{O}$ ) were calculated by the laboratory from the  $\delta^{18}\text{O}$  and  $\delta^2\text{H}$  values in sampled water. Resulting errors of the  $d$ -excess are in the order of  $\pm 1.0\text{‰}$ . All measurements were carried out following the laboratory standards which were periodically calibrated according to the international isotope water standards recommended by International Atomic Energy Agency (IAEA). The values are reported in Table 2 as per mil deviations (‰) from the V-SMOW (Vienna Standard Mean Ocean Water) standard using the conventional  $\delta$  notation [64].

Strontium (Sr) isotopic composition, namely  $^{87}\text{Sr}/^{86}\text{Sr}$  ratio, was analyzed using a VG 54E mass spectrometer (Isotopx Ltd., Cheshire, UK) and the Analyst software [65] at the Department of Mathematics and Geosciences of University of Trieste (Italy). Measured ratios were corrected for the fractionation during the analysis using the  $^{86}\text{Sr}/^{88}\text{Sr}$  ratio of 0.1194. Repeated measures ( $n = 25$ ) of the standard NBS 987 gave a mean value of  $0.710248 \pm 2$  so corrections due to the instrumental drift were not applied. Isotopic composition of the water samples are reported in Table 2.

## 4. Results and Discussion

### 4.1. Water Chemistry

The physico-chemical parameters and the major ion concentrations related to the sampled waters are presented in Table 1. Examining the data, the prevailing hydrochemical facies is the bicarbonate-calcium ( $\text{CaHCO}_3$ ) and subordinate the bicarbonate-calcium-magnesium ( $\text{Ca-Mg-HCO}_3$ ), both characteristic of waters influenced by carbonate rock dissolution processes.

The EC, as a direct expression of the water mineralization, in accordance to different water regime allows to identify different groups of water: (i) a first group characterised by a low mineralization and low EC fluctuation (Soča/Isonzo River—Is1 and Is2, Vipava/Vipacco River-Vip, Pietrarossa Lake-Pet), (ii) a second group characterised by a high mineralization and low EC fluctuation corresponding to *karst waters* from the wells/piezometers (B2 and B9), (iii) a third group characterised by a high EC fluctuation (Škocjanske jame-Sko, Abisso di Trebiciano-Tre, B4, Doberdò Lake-Dob) and (iv) a fourth group having intermediate values between the first two groups.

**Table 1.** Chemical–physical parameters and major ions chemistry with silica content. The numbers represent mean, minimum and maximum value (in parentheses) measured during the sampling surveys.

ID	T (°C)	pH	EC (S/cm)	Ca <sup>2+</sup> (mg/L)	Mg <sup>2+</sup> (mg/L)	Na <sup>+</sup> (mg/L)	K <sup>+</sup> (mg/L)	HCO <sub>3</sub> <sup>−</sup> (mg/L)	SO <sub>4</sub> <sup>2−</sup> (mg/L)	Cl <sup>−</sup> (mg/L)	NO <sub>3</sub> <sup>−</sup> (mg/L)	SiO <sub>2</sub> (mg/L)
<b>Water Cave</b>												
Škočjanske jame (Sko)	13.8 (8.1–21.9)	8.0 (7.7–8.4)	350 (297–407)	63.1 (54.4–73.3)	4.3 (3.7–4.9)	3.4 (2.9–4.0)	1.0 (0.5–1.6)	201 (173–224)	6.1 (2.7–8.0)	4.3 (2.7–5.7)	2.1 (0.0–5.3)	2.8 (0.4–3.8)
Jama v Kanjaducah (Kan)	No data	7.3 (7.2–7.5)	437.3 (371–490)	80.3 (69.1–87.9)	4.6 (4.4–4.9)	4.4 (3.5–5.4)	0.8 (0.6–1.1)	254 (214–282)	8.2 (8.0–8.7)	6.7 (5.0–8.4)	4.8 (4.5–5.5)	3.0 (2.0–4.7)
Abisso di Trebiciano (Tre)	9.8 (8.0–12.0)	7.3 (7.1–7.5)	411.3 (326–494)	78.2 (57.8–88.5)	4.6 (4.0–5.4)	5.5 (3.5–9.5)	0.8 (0.7–1.3)	244 (183–283)	9.1 (8.1–10.2)	7.8 (3.6–13.7)	5.6 (3.9–7.3)	4.0 (3.4–4.7)
Cavernetta di Comarie (Com)	13.5 (6.1–20.2)	7.5 (7.08–7.69)	359 (326–392)	58.7 (51.9–68.3)	8.3 (6.9–8.8)	3.3 (3.2–3.5)	0.7 (0.6–0.8)	206 (190–228)	7.9 (7.0–8.9)	4.3 (3.9–5.1)	6.0 (4.2–7.2)	2.6 (1.6–3.5)
<b>River</b>												
Soča/Isonzo 1 (Is1)	15.3 (9.9–23)	8.1 (7.25–8.3)	261 (231–281)	41.1 (40.0–41.8)	8.7 (7.6–9.3)	1.7 (1.3–1.9)	0.5 (0.3–0.6)	160 (153–162)	6.6 (4.3–9.3)	1.9 (1.2–2.9)	2.4 (2.2–7)	1.2 (0.9–1.6)
Vipava/Vipacco (Vip)	15.4 (6.2–26.3)	8.3 (8.1–8.4)	324 (298–352)	57.1 (49.4–64.9)	5.5 (4.7–6.1)	4.3 (3.2–6.3)	0.8 (0.6–1.0)	193 (179–207)	8.1 (7.1–10.6)	4.3 (2.9–5.4)	5.4 (3.6–8.4)	1.8 (0.9–2.9)
Soča/Isonzo 2 (Is2)	13.6 (5.3–21.2)	8.4 (8.2–8.6)	264 (250–282)	42.2 (38.8–45.5)	8.6 (7.6–9.3)	1.8 (1.3–2.3)	0.5 (0.3–0.5)	162 (154–170)	6.6 (4.6–9.5)	2.1 (1.3–3.4)	3.0 (2.1–4.2)	1.2 (0.3–2.4)
Reka (Rek)	11.6 (2.2–21.0)	8.3 (8.0–8.6)	327 (291–377)	56.0 (51.6–61.1)	5.2 (3.8–6.0)	4.2 (3.0–6.4)	1.2 (0.6–2.7)	183 (162–202)	9.7 (7.2–12.4)	4.7 (2.7–7.0)	4.0 (2.2–5.8)	2.4 (1.0–3.5)
<b>Well/Piezometer</b>												
B2			499 (476–527)	87.0 (62.1–102.2)	6.6 (5.2–8.3)	3.7 (2.6–4.8)	0.7 (0.4–1.0)	295 (270–324)	8.1 (6.8–9.1)	4.9 (2.7–6.6)	7.4 (5.1–9.6)	3.5 (2.7–3.9)
B9	15.1 (14.9–15.5)	7.2 (7.1–7.4)	471 (455–494)	85.2 (77.4–92.0)	6.0 (3.7–7.5)	4.2 (2.9–5.3)	0.5 (0.3–0.6)	277 (261–293)	7.7 (5.8–9.3)	6.4 (4.3–8.2)	4.9 (2.1–6.6)	2.7 (1.5–3.4)
P1	12.8 (12.3–13.2)	7.3 (7.2–7.3)	547 (528–585)	80.7 (75.3–86)	23.4 (21–26.4)	1.4 (1.4–1.5)	0.2 (0.2–0.2)	355 (333–376)	6.4 (6.1–6.6)	1.8 (1.7–2.0)	2.0 (1.7–2.2)	3.9 (3.4–4.6)
B4	13.9 (11.9–15.1)	7.6 (7.5–7.9)	520 (383–676)	68.7 (53.2–82.7)	10.5 (9.5–11.5)	20.5 (8.1–32.1)	1.1 (0.9–1.3)	241 (1950–280)	12.3 (9.6–14.7)	37.3 (13.5–60)	5.0 (2.5–6.5)	2.9 (2.1–4.3)
<b>Lake</b>												
Doberdò (Dob)	13.8 (10.1–13.6)	7.6 (7.4–7.7)	320 (234–376)	52.4 (30.0–63.6)	8.0 (7.1–8.8)	2.8 (2.2–3.3)	0.7 (0.6–0.8)	188 (127–220)	6.9 (4.8–8.0)	3.6 (2.5–4.4)	4.6 (0.0–6.9)	2.5 (1.9–3.1)
Pietrarossa (Pet)	13.7 (11.9–15.0)	7.7 (7.5–7.8)	338 (295–368)	54.8 (49.0–65.0)	8.1 (6.9–8.6)	3.4 (3.1–3.7)	0.6 (0.6–0.7)	195 (181–216)	7.6 (6.7–9.1)	4.6 (4.0–5.6)	4.6 (3.4–6.2)	2.1 (1.3–2.5)
<b>Spring</b>												
Aurisina (Aur)	12.5 (9.6–13.8)	7.2 (7.0–7.5)	492 (420–520)	91.5 (85.6–98.3)	4.2 (3.1–6.0)	8.5 (6.7–10.9)	1.1 (0.9–1.5)	274 (263–287)	11.4 (9.6–13.3)	14.0 (10.6–18.2)	10.4 (9.0–11.9)	2.9 (0.3–4.1)
Timavo (Tim)	12.2 (8.2–15.4)	7.4 (7.3–7.5)	420 (364–459)	75.4 (64.7–81.2)	6.7 (4.7–8.6)	5.0 (4.2–5.7)	0.7 (0.5–0.9)	244 (220–259)	8.5 (7.2–11.0)	7.9 (5.9–10.3)	6.1 (5.7–6.6)	3.2 (2.3–4.2)
Sardos (Sar)	13.3 (10.5–15.4)	7.4 (7.1–7.5)	404 (345–458)	69.0 (55.6–81.1)	8.1 (6.0–9.3)	5.0 (4.4–6.7)	0.7 (0.6–0.9)	223 (166–259)	8.5 (7.4–9.5)	7.7 (6.0–11.6)	6.2 (5.1–7.5)	2.7 (1.8–4.0)
Moschenitze N (MoN)	12.6 (10.4–14.1)	7.7 (7.4–7.6)	355 (304–385)	58.2 (50.9–69.0)	8.4 (7.3–8.8)	3.7 (3.1–4.9)	0.7 (0.6–0.8)	204 (187–228)	7.8 (7.0–8.9)	5.5 (4.0–8.7)	5.8 (4.1–6.9)	2.2 (1.2–3.2)
Moschenitze S (MoS)	13.1 (10.3–15.1)	7.5 (7.2–7.7)	407 (345–459)	70.0 (55.9–84.1)	8.0 (6.1–9.3)	5.2 (4.4–7.3)	0.7 (0.6–0.9)	234 (201–257)	8.5 (7.5–9.5)	8.2 (6.1–12.6)	6.1 (5.1–7.3)	2.7 (1.4–4.1)

The joint analysis of the EC along with the  $Mg^{2+}/Ca^{2+}$  molar ratio (Figure 3), evidenced that most of the analyzed points lie along a regression line, the end-members of which are represented by the Soča/Isonzo waters (Is1 and Is2) in one end and the waters from Aurisina Spring (Aur) and the piezometers (B2 and B9) at the other end. Outside from the regression line are placed waters from piezometers (P1, B4), Reka, Škočjanske jame (Sko) and Vipava/Vipacco rivers (Rek and Vip).

Groundwater collected in P1 has similar EC value to the waters collected in the other piezometers, but it clearly differs in the  $Mg^{2+}/Ca^{2+}$  molar ratio, where it shows the highest values. The high  $Mg^{2+}/Ca^{2+}$  molar ratio can be justified by the dolomitic formation in which the piezometer was drilled (Figure 1(No. 27)).

Water from B4 shows a different behavior according to the water regime: during extreme low flow conditions (Figure 3a) it shows values similar to the ones of Moschenizze North and Sardos springs (MoN and Sar), while during floods (Figure 3b,c), it has very high EC values due to the mixing with salt marine waters [66].

The Reka River (Rek—a monitored water point in correspondence of the surface waters of the Reka River) and Škočjanske jame (Sko—the swallow hole of the Reka River) waters, as expected, have a specific sign which shows always low EC and an average  $Mg^{2+}/Ca^{2+}$  molar ratio of about 0.10–0.18 which are the expression of waters flowing on a flysch and carbonate watershed.

Water from Abisso di Trebiciano (Tre) demonstrates different behavior: during low flow (Figure 3a), it remains on the line, while during floods (Figure 3b,c), as expected, the water collected in the cave has a mineralization similar to the ones of Rek and Sko, which means that during low flow, Tre is draining mainly *karst waters* and is poorly influenced by Reka River, which in turn instead prevails during floods.

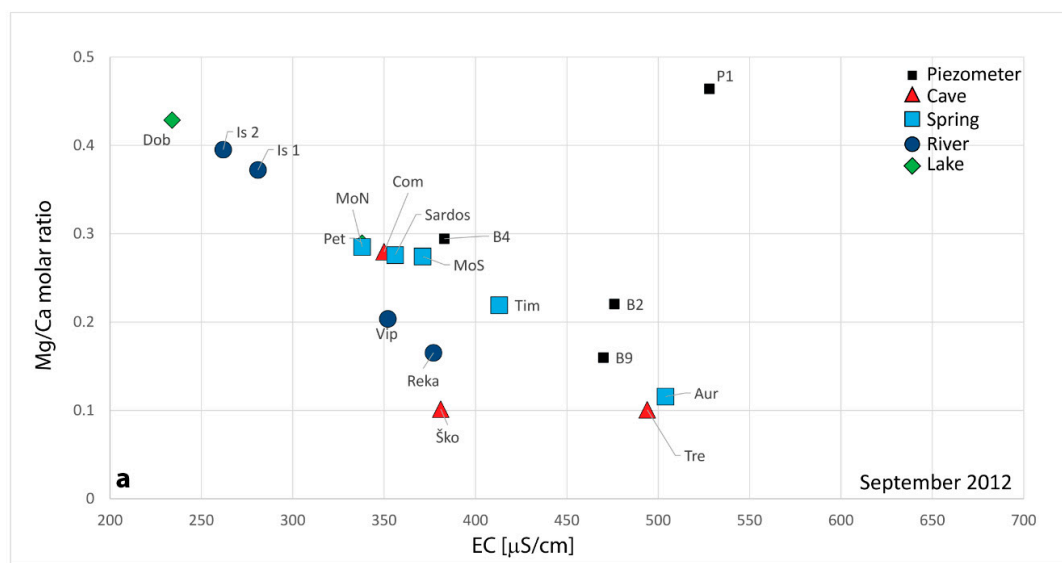
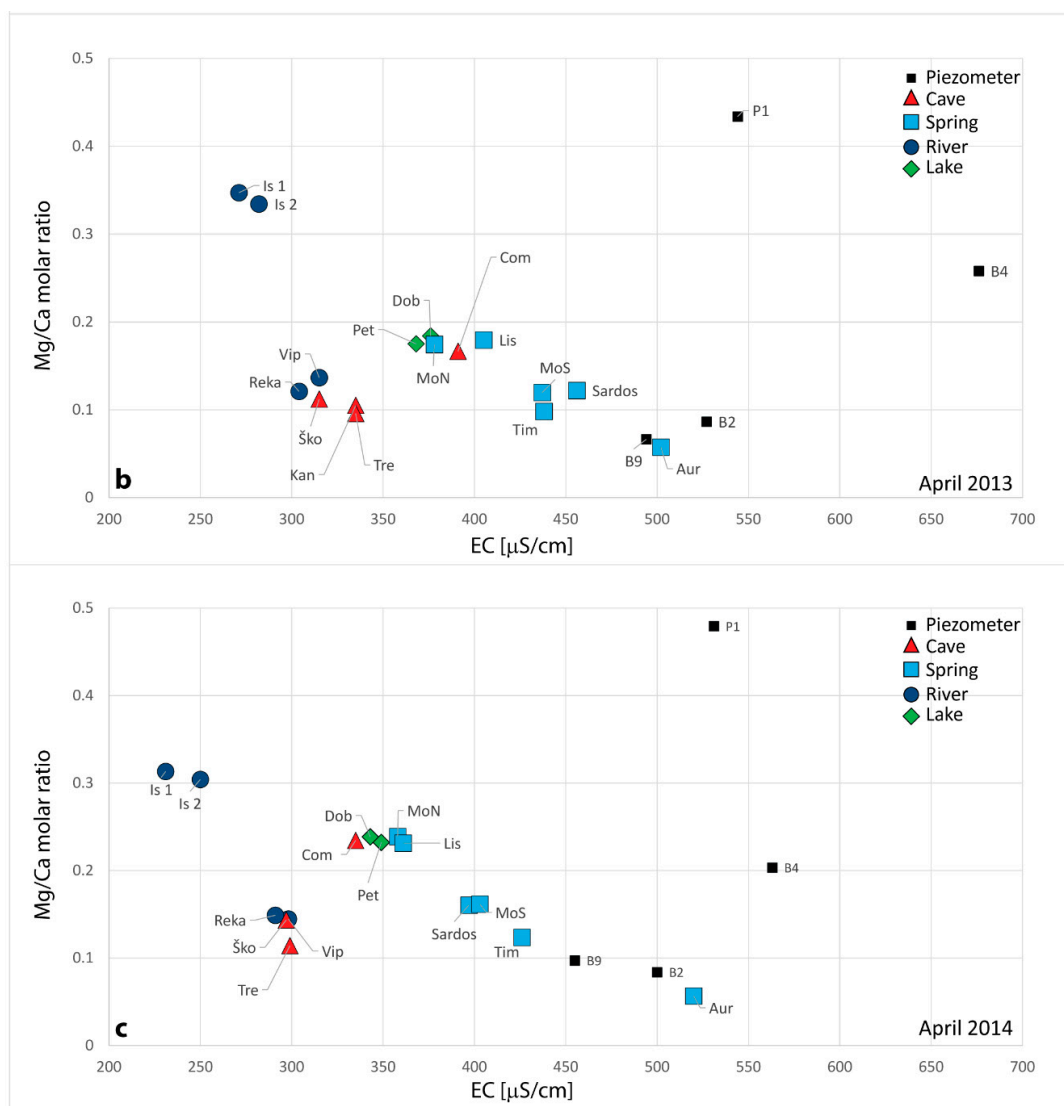


Figure 3. Cont.





**Figure 3.** Electrical Conductivity (EC) ( $\mu\text{S}/\text{cm}$ ) versus  $\text{Mg}^{2+}/\text{Ca}^{2+}$  molar ratio. The figure represents three specific hydrogeological conditions: (a) extreme low flow; (b) decreasing limb of a high flood; (c) decreasing limb of a moderate flood.

4.2. Environmental Isotopes: Xygen and Hydrogen Isotopic Composition ( $\delta^{18}\text{O}$  and  $\delta^2\text{H}$ )

Table 2 summarizes the isotopic composition of  $\delta^{18}\text{O}$ ,  $\delta^2\text{H}$ , *d*-excess minimum and maximum values,  $^{87}\text{Sr}/^{86}\text{Sr}$  and Sr in the sampled waters (for Sr the mean value was added).

**Table 2.** Minimum and maximum values of  $\delta^{18}\text{O}$ ,  $\delta^2\text{H}$ , *d*-excess, strontium isotope ratio ( $^{87}\text{Sr}/^{86}\text{Sr}$ ). Mean, minimum and maximum Sr content in sampled waters.

ID	$\delta^{18}\text{O}$ (‰)	$\delta^2\text{H}$ (‰)	<i>d</i> -Excess (‰)	$^{87}\text{Sr}/^{86}\text{Sr}$	Sr ( $\mu\text{g}/\text{L}$ )
<b>Water cave</b>					
Škočjanske jame (Sko)	−5.25	−37.6	4.4	0.708105	98.3
	−8.86	−56.0	14.9	0.708450	(79.1–120.9)
Jama v Kanjadučah (Kan)	−7.40	−46.0	13.2	0.707580	316.4
	−8.41	−52.3	15.0	0.708012	(273.7–359.1)
Abisso di Trebiciano (Tre)	−7.47	−46.3	13.3	0.707487	238.9
	−8.58	−54.0	15.5	0.708071	(81.8–552.4)

Table 2. Cont.

ID	$\delta^{18}\text{O}$ (‰)	$\delta^2\text{H}$ (‰)	<i>d</i> -Excess (‰)	$^{87}\text{Sr}/^{86}\text{Sr}$	Sr ( $\mu\text{g/L}$ )
Cavernetta di Comarie (Com)	−8.02	−50.5	13.7	0.707738	104.5
	−8.95	−55.9	15.7	0.707930	(91.5–120.2)
<b>River</b>					
Soča/Isonzo 1 (Is1)	−8.38	−52.9	14.1	0.708094	50.1
	−9.50	−60.9	15.7	0.708700	(39.8–55.4)
Vipava/Vipacco (Vip)	−7.86	−49.0	13.1	0.707596	124.8
	−9.00	−57.3	14.7	0.708300	(88.2–214.4)
Soča/Isonzo 2 (Is2)	−8.33	−52.4	14.2	0.708076	46.8
	−9.42	−60.2	15.7	0.708370	(11.5–63.9)
Reka (Rek)	−5.92	−38.3	9.1	0.708295	93.6
	−8.89	−56.4	14.9	0.708530	(82.2–121.5)
<b>Well/Piezometer</b>					
B2	−6.90	−42.6	12.6	0.707508	171.4
	−7.55	−46.5	13.9	0.707815	(110.8–231.6)
B9	−7.13	−43.8	13.0	0.707508	278.9
	−7.61	−46.1	15.0	0.707540	(225.1–406.3)
P1	−6.92	−42.8	12.4	0.707362	82.2
	−7.26	−43.7	15.3	0.707800	(17.2–125.9)
B4	−7.37	−45.5	13.3	0.707602	265.1
	−8.62	−53.7	15.3	0.707910	(164.3–351.8)
<b>Lake</b>					
Doberdò (Dob)	−6.90	−45.8	9.4	0.707925	86.2
	−8.88	−54.5	16.5	0.708530	(54.7–101.1)
Pietrarossa (Pet)	−8.09	−50.7	13.3	0.707684	135.4
	−9.05	−57.5	14.9	0.707815	(119.7–167.2)
<b>Spring</b>					
Aurisina (Aur)	−7.18	−43.7	13.0	0.707603	165.1
	−7.99	−49.3	14.6	0.708190	(86.5–341.8)
Timavo (Tim)	−7.62	−46.8	14.4	0.707589	192.4
	−8.56	−52.3	16.2	0.708210	(59.6–299.6)
Sardos (Sar)	−7.67	−48.3	13.0	0.707695	191.9
	−8.63	−52.6	16.4	0.707840	(152.7–227.8)
Moschenizze North (MoN)	−8.02	−49.7	13.0	0.707872	105.4
	−8.85	−55.6	15.2	0.708670	(92.0–124.8)
Moschenizze South (MoS)	−7.65	−47.0	12.7	0.707659	187.1
	−8.64	−52.9	16.2	0.707725	(153.4–214.0)
<b>Pluviometer</b>					
Sela na Krasu	−3.51	−18.7	9.4	No data	No data
	−9.34	−61.2	14.8	No data	No data
Klariči	−4.00	−20.3	7.7	No data	No data
	−8.94	−58.2	14.3	No data	No data
Filzi (Trieste)	−4.16	−22.7	7.5	No data	No data
	−10.01	−66.7	13.3	No data	No data
Basovizza	−5.71	−32.2	7.3	No data	No data
	−10.89	−79.5	13.8	No data	No data
Randaccio	−4.33	−27.6	7.0	No data	No data
	−9.26	−61.3	13.0	No data	No data
Gorizia	−4.10	−25.6	7.2	No data	No data
	−7.60	−49.1	13.3	No data	No data

Within the three-year project, in total, a 125 water samples from surface, cave and spring waters as well as the waters of the piezometers were collected for the isotope analysis of  $\delta^{18}\text{O}$ ,  $\delta^2\text{H}$  and *d*-excess, respectfully.

Precipitation data collected in correspondence of the pluviometers in Klariči and Sela na Krasu (on Slovenian side) and Gorizia, Randaccio, Trieste and Basovizza (on Italian side), were analyzed for  $\delta^{18}\text{O}$ ,  $\delta^2\text{H}$ , *d*-excess within the study period. The isotopic composition of the precipitation ranges between −10.89 and −3.51‰ for  $\delta^{18}\text{O}$ , and between −79.5 and −18.7‰ for  $\delta^2\text{H}$  (Figure 4).

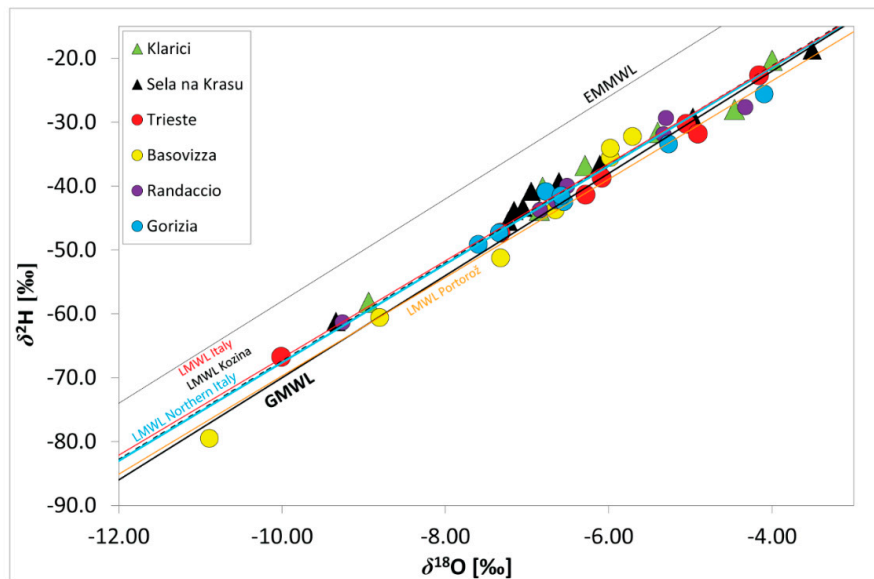


Figure 4.  $\delta^{18}\text{O}$  versus  $\delta^2\text{H}$  isotopic values of the precipitation samples collected in the pluviometers.

Isotopic composition of  $\delta^{18}\text{O}$  in precipitation is predominantly more depleted (more negative) during colder months (winter) and enriched in the summer. Measured values indicate that the isotopic composition of observed precipitations falls on the Global Meteoric Water Line (GMWL) defined by Craig [67] and various Local Meteoric Water Lines (LMWLs) defined for Italy [68] and Slovenia (locations Kozina and Portorož [69,70]) and are always plotted below the Eastern Mediterranean Meteoric Water Line (EMMWL, [71]). The minimum *d*-excess value found in the study area is 7.0‰ measured in May 2014 at Randaccio and a maximum value of 14.8‰ measured in November 2013 at Sela na Krasu (Figure 2, Table 2). Randaccio is situated practically at sea level, while the pluviometer at Sela na Krasu is sited at approximately 270 m a.s.l., so Sela na Krasu precipitation values are therefore more  $^{18}\text{O}$  depleted.

Previous studies on *d*-excess showed that values of 14‰ are typical of the western part of the Mediterranean basin, while an excess of 22‰ reflects a mixture between the Mediterranean and the Atlantic air masses [69,72]. Overall measured values suggest the influence from Mediterranean air masses having *d*-excess values around 10‰ [73–76]. With respect to the precipitations, the results of the present research substantially confirm the previous studies [6,28,31–34,36].

The isotopic composition of oxygen in sampled water (precipitation excluded) varies between  $-9.50$  and  $-5.25$ ‰, while the hydrogen one ranges between  $-60.9$  and  $-37.6$ ‰, and *d*-excess ranges between 4.4 and 16.5‰.

The graphs  $\delta^{18}\text{O}$  versus  $\delta^2\text{H}$  (Figure 6a–c) show small deviation from the GMWL. In fact, majority of water samples fall between GMWL and EMMWL as previously defined also for the precipitations (Figure 4). Water samples are plotted closely along the already identified LMWL determined for precipitation in Slovenian Kozina [69], Italy and Northern Italy [68].

As a rule, the isotopic composition of precipitation changes with the elevation and becomes always more depleted in  $^{18}\text{O}$  and  $^2\text{H}$  at higher altitudes [77]. This represents one of the most useful applications in isotope hydrology, namely the identification of the elevation at which groundwater recharge takes place. The situation is well represented in Figure 4 where precipitations fall on the line comparable to the altitude effect determined for the Coastal and Alpine region with the value from  $-0.22$  to  $-0.25$ ‰  $\delta^{18}\text{O}/100$  m [78,79]. The sampled points representing the *karst waters* (P1, B9 and B2) fall on a line having the same gradient. All the other points do not have the same behavior, but are distributed between Soča/Isonzo River values and the piezometers. On the left part of the graph, more depleted  $\delta^{18}\text{O}$  values are encountered representing the surface waters of the Soča/Isonzo

River. It is well known that its recharge basin is located at higher altitudes. Its springs in fact are at 990 m a.s.l., in the Slovenian Trenta Valley, in the Julian Alps at the bottom of Travnik Mt. (2320 m a.s.l.). For this reason, Soča/Isonzo River (Is1 and Is2) always has more depleted values than all the other samples, especially during the springtime when usually the important snowmelt contributes to the river discharge. Lakes as Doberdò (Dob) and Pietrarossa (Pet), as in the other analyses, clearly seems to be affected by the influence character of the Soča/Isonzo River seen their  $\delta^{18}\text{O}$  values always lower than  $-8.0\text{‰}$ . All the other water observation points present values in between, witness of a mixing effect among different contributions is difficult to be explained considering only mean data.

Observing  $d$ -excess values in sampled waters (Table 2), higher  $d$ -excess values are mostly related to depleted  $^{18}\text{O}$  values, showing a significant altitude effect that increases with the altitude, as indicated in the case of  $\delta^{18}\text{O}$  (Figure 5). Similar results were observed by Roller-Lutz et al. [80] for the area of Rijeka Bay in Croatia. On the other hand, water from Škocjanske jame (Sko) has different behaviour than the other water points, since it has low  $d$ -excess and is enriched in  $^{18}\text{O}$ . This could be due to occurrence of isotope evaporation effect on the Reka River. From its spring up to Škocjanske jame the Reka River flows on the surface where quite intensive evaporation could be expected, especially during warmer months.

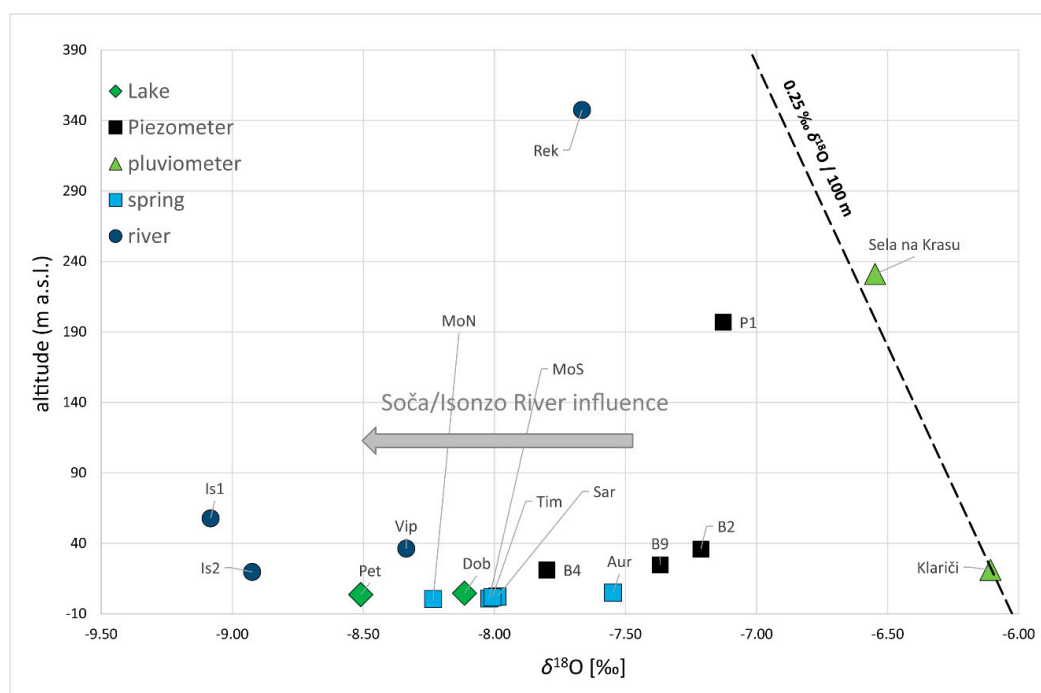


**Figure 5.** Isotopic composition of mean  $\delta^{18}\text{O}$  versus the altitude of the sampling locations. The two green triangles represent the precipitations data collected in correspondence of Klariči and Sela na Krasu pluviometers. The obtained isotopic gradient is in accordance with the values of Michelini [78] of  $-0.22\text{‰ } \delta^{18}\text{O}/100\text{ m}$  and Mezga et al. [79] of  $-0.25\text{‰ } \delta^{18}\text{O}/100\text{ m}$ .

Analyzing the data of  $\delta^{18}\text{O}$  versus  $\delta^2\text{H}$ , during different hydrogeological regimes (Figure 6a—low flow, 6b—high flood and 6c—moderate flood) different behaviors emerge. The water from piezometers B2, B9 and P1 is always enriched in  $^{18}\text{O}$  (less negative values), close to the ones characteristics of the local precipitations (Klariči mean  $\delta^{18}\text{O}$  is  $-6.11\text{‰}$  and Sela na Krasu mean  $\delta^{18}\text{O}$   $-6.53\text{‰}$ ). It can be affirmed that the piezometers represent the right end-member of the mixing line. The other end-member is defined by the Soča/Isonzo River (Is1 and Is2) sampled waters, which are instead always more depleted (more negative values) than all the other values.

During low flow conditions (Figure 6a) some points (Dob, Rek and Sko), deviate from the mixing line, remaining always beneath the LMWL of Northern Italy. As Horton et al., [81] testify, the deviation can be explained with the evaporation process being these water points a lake (Dob), a river (Rek) with a very low discharge at the moment of sampling ( $0.5 \text{ m}^3/\text{s}$ ), and the swallow hole of the Reka River (Sko) in a torrid summer during which no precipitations occurred for a long time before the sampling survey (2 months is a long time for the latitudes at which the Classical Karst Region is).

The deviation in fact is completely absent in the samples collected during the springtime, during floods (Figure 6b,c). The samples collected in 2013 and 2014 are clearly aligned and in general more depleted. During floods, the contribution due to Reka River is hidden being characterised by isotopic values in between Soča/Isonzo River and karst waters (P1, B2, B9). During low flow conditions, instead, when the discharge is  $12$  to  $10 \text{ m}^3/\text{s}$  at the Timavo springs, the Reka River discharge consists only in few hundreds of  $\text{L}/\text{s}$  ( $0.5 \text{ m}^3/\text{s}$ ) and does not influence, in a meaningful way, the geochemistry of the monitored waters (Figure 6a).

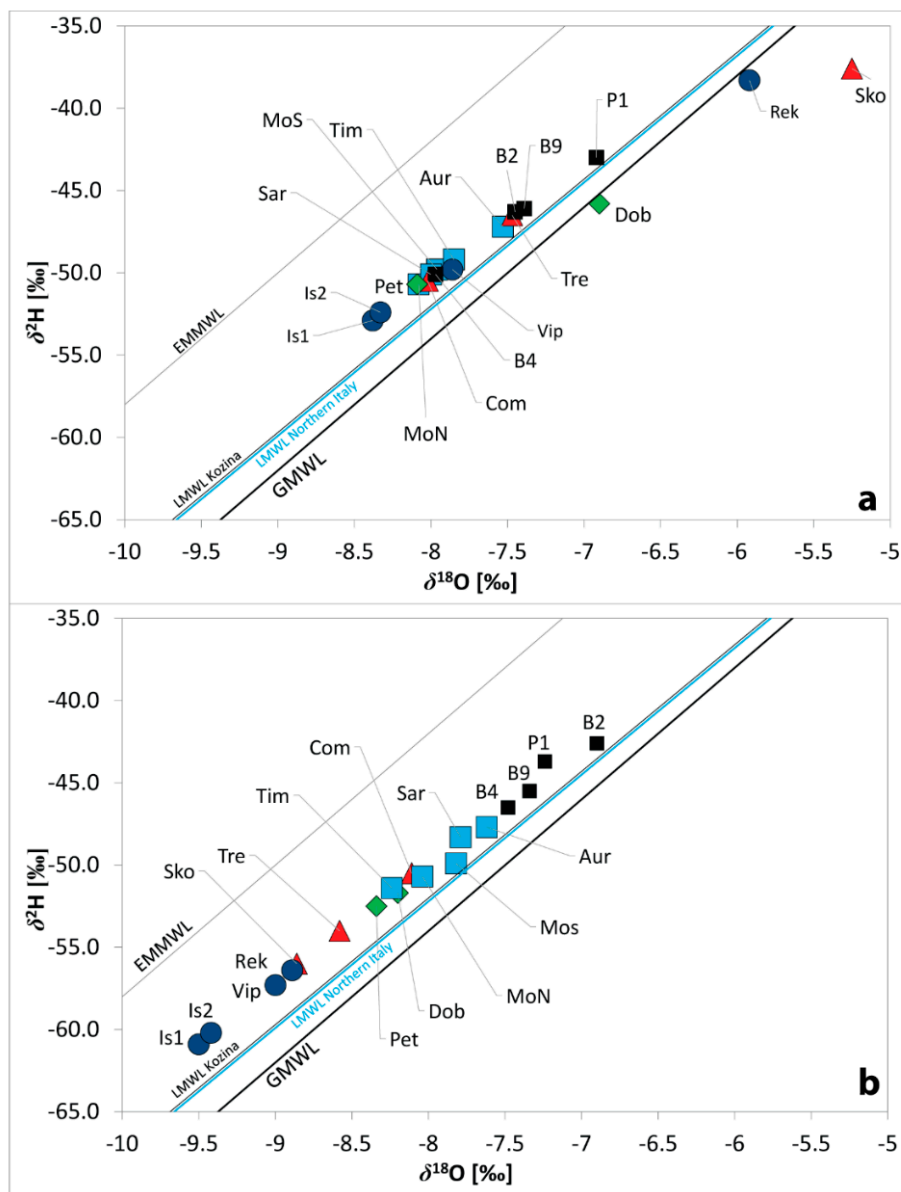
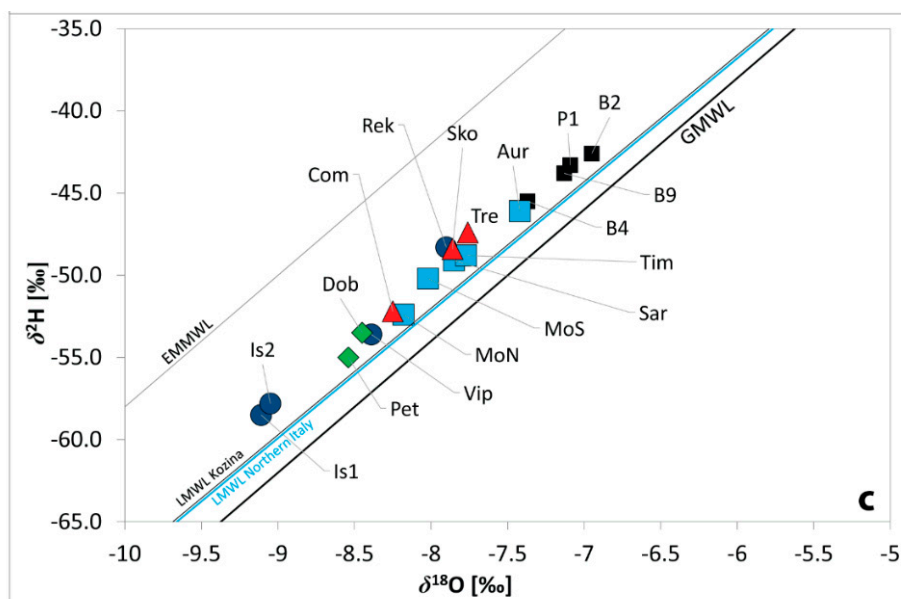


Figure 6. Cont.



**Figure 6.**  $\delta^{18}\text{O}$  versus  $\delta^2\text{H}$  isotopic values of the samples collected: (a) results related to data collected in September 2012 during extreme low flow conditions; (b) results related to data collected in April 2013 in correspondence of the decreasing limb of a high flood; (c) results related to data collected in April 2014 in correspondence of the decreasing limb of a moderate flood. Legend for Figure 6a–c Blue circles represents the surface waters, black squares are related to the piezometers, springs are in sky-blue square and caves in red triangle. The reference meteoric water lines as GMWL [67], Eastern Mediterranean Meteoric Water Line (EMMWL [71]) and Local Meteoric Water Lines (LMWLs) defined for Slovenia (Kozina) [69] and Northern Italy [68] are shown.

When comparing the chemical data with the isotopical data, a similar result to the one emerged from the analysis of Figure 3 is observed. The relation between  $\text{HCO}_3^-$  and  $\delta^{18}\text{O}$  values (Figure 7) can discriminate the possible contributions to the mixing waters within the karst hydrostructure.

Generally, most of the water samples fall along the line linking *karst waters* (B2, B9 and P1) to Soča/Isonzo River component, which represent the two end members: *karst waters* are enriched in  $\text{HCO}_3^-$  and heavy oxygen isotope, while Soča/Isonzo River component is, on the other side, depleted on both parameters. Some differences can be noticed while analyzing the different sampling periods. As occurred also examining the graph EC versus  $\text{Mg}^{2+}/\text{Ca}^{2+}$  molar ratio (Figure 3), on September 2012 (Figure 7a) Dob, Rek and Sko represent the outliers with very low  $\delta^{18}\text{O}$  values due to the summer evaporation. Their values in fact remain closer to the mixing line while analyzing different periods as April 2013 and April 2014. In addition, the waters sampled in correspondence of Trebiciano Abyss (Tre) have a particular behavior according to the water regime. In the sampling survey of September 2012, Tre waters have values characteristics of *karst waters*, completely different from the ones of the Reka River or of the Škocjanske jame defining that during low flow conditions *karst waters* are the ones which flow through Trebiciano Abyss. The sampling done in April 2013 (Figure 7b), realized on the decreasing limb of a high flood occurred after a period of intense rainfalls over the karst area, shows that Tre has values that differ from the ones of Rek and Sko, witnessing an important contribution of the *karst waters* which have always higher  $\text{HCO}_3^-$  and  $\delta^{18}\text{O}$  values. This contribution is even more meaningful if we look at Timavo Spring (Tim) which has higher  $\text{HCO}_3^-$  and  $\delta^{18}\text{O}$  values.

The sampling realized on April 2014 (Figure 7c) on the decreasing limb of a moderate flood highlights that Sko, Tre and Rek have the same values, with a low  $\text{HCO}_3^-$  content which implies that during floods Tre is draining Rek and Sko waters which quickly reach the inside of the hydrostructure being, in turn, more significant than the contribution due to the *karst waters* on the karst area.

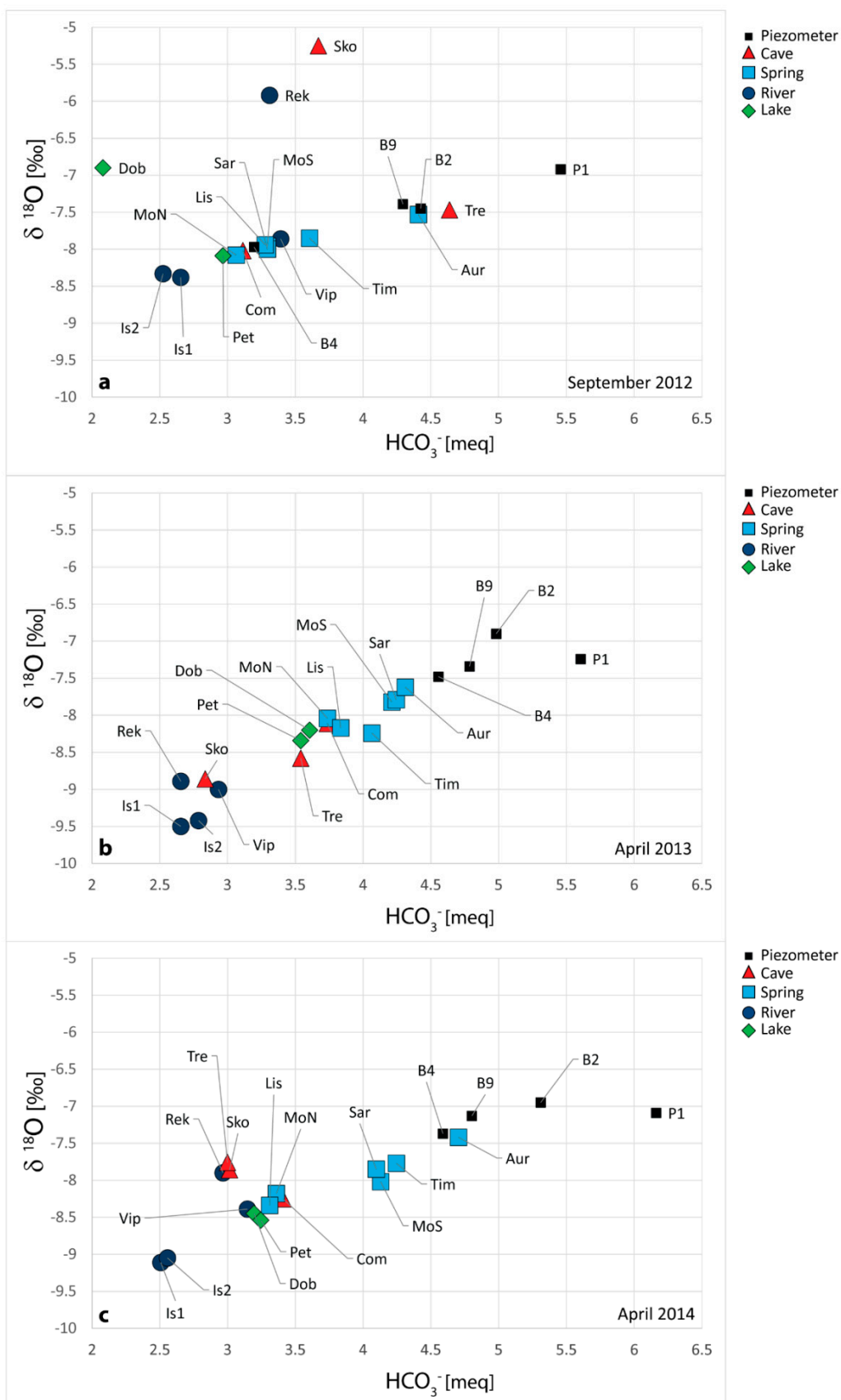


**Figure 7.**  $\text{HCO}_3^-$  (meq) versus  $\delta^{18}\text{O}$  (‰). The figure represents three specific hydrogeological conditions: (a) extreme low flow; (b) decreasing limb of a high flood; (c) decreasing limb of a moderate flood.

#### 4.3. Environmental Isotope: Strontium Isotope Ratio ( $^{87}\text{Sr}/^{86}\text{Sr}$ )

Unlike the oxygen and hydrogen, strontium (Sr) is a non-conservative element, which means that the isotopic concentration and composition varies according to the rock-water interaction: if the interaction time is long, the water tends to reach the isotopic equilibrium with the rock. Even if this technique is widely adopted in hydrogeology [2,5,82–94], for the Classical Karst Region waters no references can be found until now. So, data concerning the strontium isotope ratio ( $^{87}\text{Sr}/^{86}\text{Sr}$ ) in Classical Karst Region waters are here presented for the very first time.

From the data analyses (Table 2 and Figure 8) emerge that Soča/Isonzo and Reka rivers have a similar isotopic composition of the Sr element ( $^{87}\text{Sr}/^{86}\text{Sr}$ ), on average higher than all the other analyzed water samples. The waters of these two rivers, infiltrating into the hydrostructure, gradually interact with the carbonate rocks which have a lower Sr isotopic composition. For this reason, the strontium isotopic ratio ( $^{87}\text{Sr}/^{86}\text{Sr}$ ) tends to decrease trying to reach the equilibrium with the carbonate rocks. Springs, piezometers and cave waters show intermediate values between the strontium isotopic composition ( $^{87}\text{Sr}/^{86}\text{Sr}$ ) of Soča/Isonzo and Reka rivers and the ones of a *karst water* in equilibrium with the Cretaceous carbonate rock (limestone) present in the study area having an average Sr isotopic composition of 0.70750 (Figure 8).

Observing the water samples collected in the area within the three-year project, it can be concluded that all the analyzed waters indicate a mixing process between a component tending to an equilibrium with the carbonate rocks (with a low Sr isotopic composition and a high Sr content) and a component tending to an equilibrium with the silica minerals having a higher radiogenic ratio and a lower Sr content as the waters coming from Soča/Isonzo and Reka rivers. The three different situations analyzed (Figure 8a–c) show in turn a complex behavior of the waters according to the specific water regime. During low flow conditions in fact, when Reka River has a very low discharge not influencing the aquifer recharge, Tre and B9 represent one of the two end members of a binary mixing line of which the other end is occupied by Soča/Isonzo waters. The regression line shows a very high  $R^2$  value of 0.90. The situation differs while analyzing the samples collected in the decreasing phase of floods (Figure 8b,c): the values are definitively more disperse, the regression lines shows very low correlation values ( $R^2 = 0.45$  in Figure 8b;  $R^2 = 0.55$  in Figure 8c) not only allowing for identifying two end members, but also suggesting the presence of more inputs to the outflows. Especially in Figure 8c, on the left end can be identified the contribution due to the *karst waters* represented by the waters collected in the piezometers. On the other end, the presence of the Reka and Soča/Isonzo rivers is not very distinctive since their very similar values do not allow the definition of their specific contribution to the outflows.



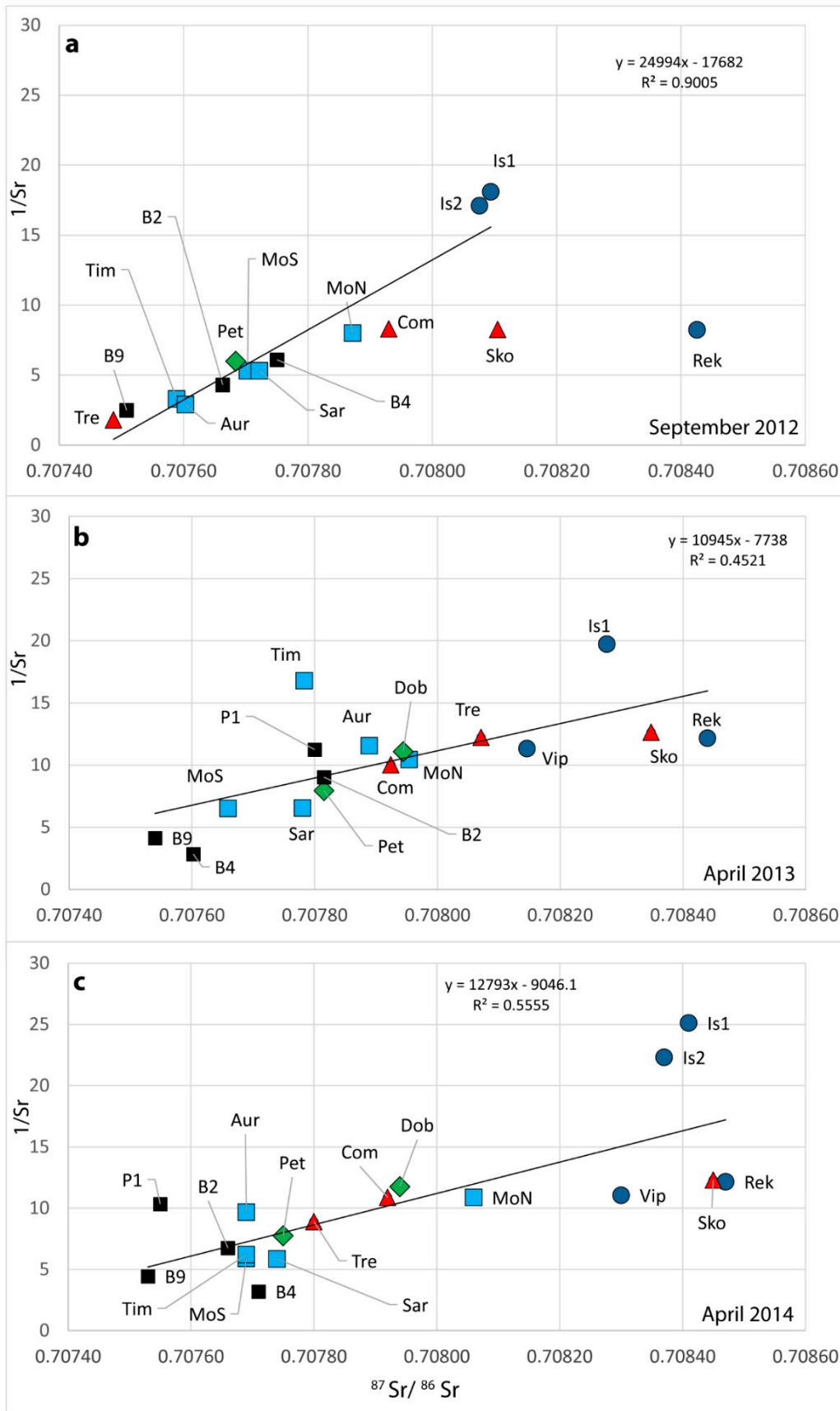


**Figure 8.**  $^{87}Sr/^{86}Sr$  versus  $1/Sr$  analyzed during three different water regimes: (a) low flow; (b) decreasing limb of a high flood; (c) decreasing limb of a moderate flood.

Comparing the isotopic ratios  $^{87}\text{Sr}/^{86}\text{Sr}$  and the  $\delta^{18}\text{O}$  values related only to the sampling survey of April 2014 (Figure 9), it is instead possible to quantify the contribution of the Reka and the Soča/Isonzo rivers to the different outflows during floods. The curves proposed in Figure 9, show the evolution of the mixing between three components:

- (1) A water in equilibrium with the carbonate rocks for the Sr isotopic composition ( $^{87}\text{Sr}/^{86}\text{Sr} = 0.70750$ ) and the  $\delta^{18}\text{O}$  isotopic composition similar to the mean local rainfalls ( $\delta^{18}\text{O} = -7.2\text{‰}$ );
- (2) Soča/Isonzo River ( $\delta^{18}\text{O} = -9.05$ ,  $^{87}\text{Sr}/^{86}\text{Sr} = 0.70837$ );
- (3) Reka River ( $\delta^{18}\text{O} = -7.86$ ,  $^{87}\text{Sr}/^{86}\text{Sr} = 0.70847$ ).

Data highlight a clear influence of the Reka River at Škocjanske jame, Abisso di Trebiciano and at the Aurisina springs (Figure 9, upper line).

Water from piezometers present enrichment in heavy isotopes (less negative  $\delta^{18}\text{O}$  values) and a low  $^{87}\text{Sr}/^{86}\text{Sr}$  ratio which is compatible with waters that remained for a long time in contact with the carbonate bedrock highlighting a slower circulation within the fissures and a clear contribution to their recharge due to the local effective infiltrations (*karst waters*).

Concerning the contribution given by Soča/Isonzo River, it is definitively clear for Pietrarossa Lake.

All the water points falling within the two mixing curves show a more complex recharge, not only binary.

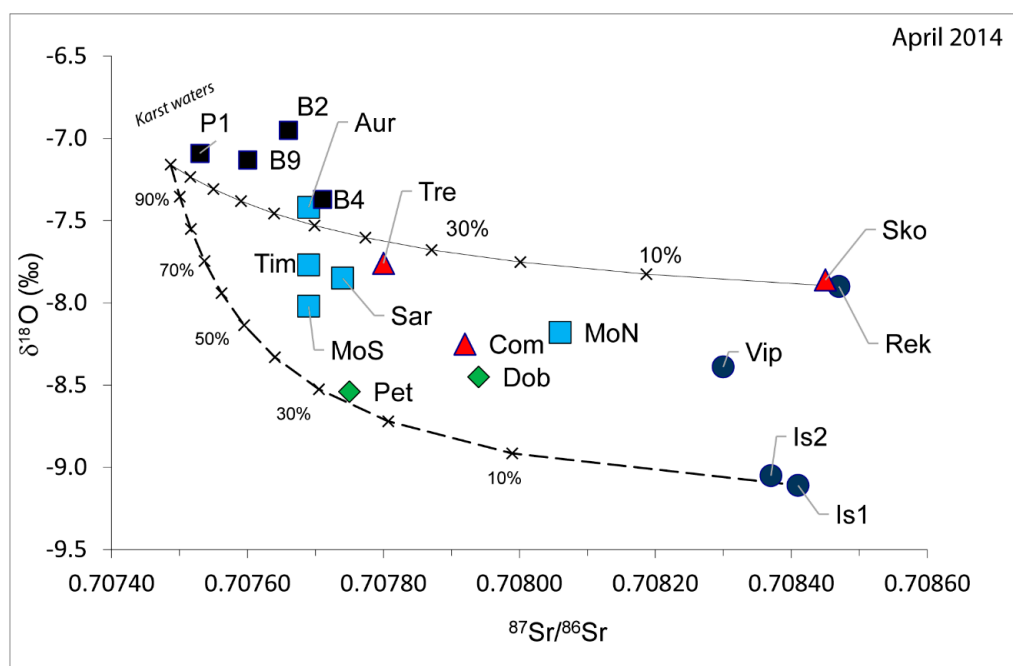


**Figure 9.** Isotopic ratio  $^{87}\text{Sr}/^{86}\text{Sr}$  versus the  $\delta^{18}\text{O}$  (‰) values in water samples from April 2014. The dashed line represents a mixing line between waters having characteristics in between *karst waters* and Soča/Isonzo River waters; the continuous line instead, represents a mixing line between waters having characteristics in between *karst waters* and Reka River waters.

During low flow conditions, as it occurred in 2012, the system is easier to understand and it is possible to estimate the recharge contribution to the springs.

During low flow conditions, one of the components has the value of the sampled waters in Trebiciano Abyss and the other component has the value of Soča/Isonzo River in correspondence of Is2. Applying the rule exposed by Hogan et al. [95] and Négrel et al. [96], at Com we have the 97%,

at Sar 90%, at MoN 95%, at MoS 85%, at Pet 83%, at Tim 66%, at B2 80%, at B4 88%, at B9 26% of Soča/Isonzo influence. The result is partially in agreement with the results obtained by Calligaris et al. [44] using the Electrical Conductivity to define the percentages of the difference contributions at the outflows. This method is applicable if the only meaningful differences in the ion composition are due to the concentration of calcium bicarbonate. The obtained values for the period 2015–2016 (a period different from the one of the project) have been, on average, lower than 15% with respect to the period considered during the project.

Summarizing, data available allowed to define different behavior of the waters at the springs, characteristics of the two extreme hydrogeological regimes. During low flow conditions, two are the contributions which recharge the springs: Soča/Isonzo waters and *karst waters*. In these hydrogeological conditions, the discharge of the Reka River is very low and its contribution to the analyzed water points is not meaningful. Not only the chemical analyses, but also the isotopical ones allow for distinguishing only these two contributions (Figures 3a, 6a, 7a and 8a). Moving in the spring area, from east (Aurisina Spring) to west (Pietrarossa springs), there is an initial prevailing of *karst waters* which in turn are replenished by the waters of the Soča/Isonzo River (Figure 10).

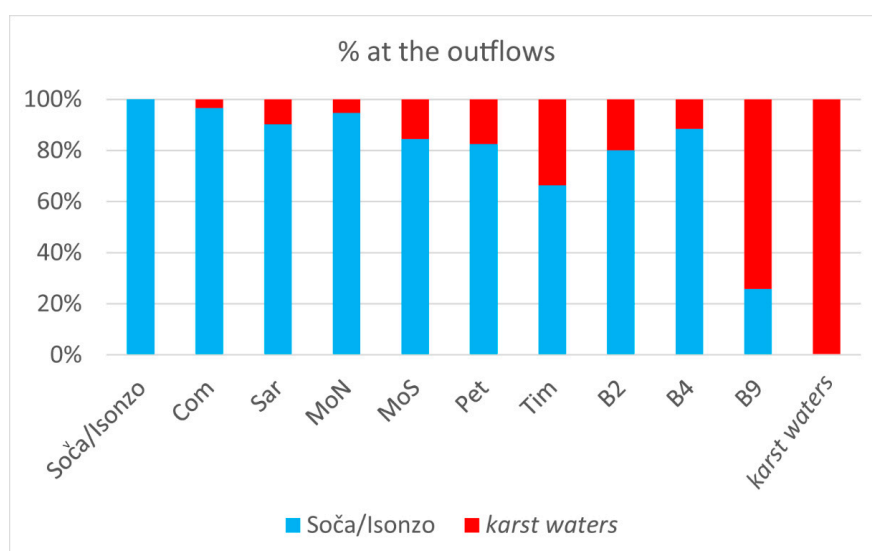


**Figure 10.** The mixing (%) between waters from Soča/Isonzo River (Is2) and *karst waters* (effective infiltrations) for the water samples collected during low flow conditions in September 2012.

During floods instead, the contribution due to Rek become important but it is not possible to quantify it only using the chemical analyses and the stable isotopes. In the system in fact are present at least three contributions which can be distinguished thanks to the joint analyses of conservative and non-conservative isotopes (Figure 9). As already highlighted by several dye-tests realized in the area ([27] and all the references within), the Rek contribute to the discharge of Tre, Aur and Tim. But, while Tre and Aur are placed very close to the mixing line between Rek and *karst waters*, Tim deviate on values similar to the ones of Sar and MoS (Figure 9) indicating the presence of a third contribution.

During floods, the contribution due to the Is1 and Is2 is instead visible at Pet. The other points, falling in between the two mixing lines (Dob, Com and MoN), have isotopical values among Rek, Is1 and Is2, and *karst waters*. All the evidences from the previous studies and especially the experiences with the dye-tests, testify that Rek influences only the eastern springs up to Sar and MoS. We can exclude that there can be an influence of the Rek on Dob, Com and MoN. This highlights the limit of the applied methodologies, or the presence, during floods of a different contribution which can be represented by waters similar to the ones of Vip. Previous authors agree ([19] and all the references

within) on the poor contribution due to the Vip to the water points recharge, raising an open question which will require more detailed studies in the future.

## 5. Conclusions

Although groundwater from the shared cross-border Classical Karst Region aquifer is no longer a primary source used for drinking water for the Italian side, it is still a resource for the Slovenian one (Klariči). The hydrogeological complexity of this zone represented a challenge for the researchers, which are for more than hundred years trying to fully understand the groundwater flow contributions to the springs. The present study, conducted in the framework of HYDROKARST 3-years European project, provided the possibility to access and sample some difficult accessible locations in Italy and Slovenia, to analyze the waters for geochemical parameters, especially Sr and Sr isotope ratios for the very first time. The sampling over a certain time-period in different hydrogeological regimes, gave the possibility to understand and to quantify the different contributions of the recharge components to the spring areas, helping to interpret the actual hydrogeological conditions and to delineate future cross-border activities to safeguard and sustainably manage valuable groundwater resources.

More than 100 water samples collected from precipitations, surface waters, springs, caves, wells and piezometers gave the possibility to have a good qualitative overview of the whole area, with results that mostly confirmed the past findings on the general hydrogeology of the area.

The precipitation monitoring network was implemented with respect to the past studies- covering especially the western side of the Classical Karst Region. The obtained results for the stable oxygen and hydrogen isotopic composition proved a predominant influence from Mediterranean air masses. Precipitation data is in accordance with the previous studies with the isotopic gradient varying between  $-0.22$  and  $-0.25\text{‰}$   $\delta^{18}\text{O}/100$  m.

Regarding the different contributions to the recharge, previous studies delineated the overall idea: the aquifer is recharged by the effective precipitations, the Reka River which is swallowed into the Škocjanske jame sinkholes and by the leakages of the Soča/Isonzo and Vipava/Vipacco rivers. The aim of the present research was to quantify the different contributions of the recharge to the discharge at the different water points in different hydrogeological regimes, combining the classical chemical analyses with conservative and non-conservative isotopical ones (if has never been done before).

Data available allowed defining two different behavior of the waters at the springs, characteristics of the two extreme hydrogeological regimes. During low flow conditions, two are the contributions which recharge the springs: Soča/Isonzo waters and *karst waters*. During floods instead, the contribution due to Reka River become important but it is not possible to quantify it only using the chemical analyses and the stable isotopes. In the system in fact are present at least three contributions which can be distinguished thanks to the joint analyses of conservative and non-conservative isotopes. As defined by several dye-tests realized the Reka River contribute to the discharge of Trebiciano Abyss, Aurisina and Timavo springs. But, while Trebiciano Abyss and Aurisina are placed very close to the mixing line between Reka River and *karst waters*, Timavo deviates on values similar to the ones of Sardos and Moschenizze South indicating the presence of a third contribution. Even if past Authors agree on the poor contribution due to Vipava/Vipacco River, the analyses of the isotopic Sr ratio makes its contribution as an open question for future and more detailed studies in this complex underground karst system.

Specific studies are required also for the well B4 which is a tapped point of the Slovenian Klariči drinking water supply. During low flow conditions, the waters in B4 are mainly influenced by Soča/Isonzo waters and secondary by *karst waters*. During floods, instead, the pumping well shows a completely different behavior from all the other points which is due to the contribution of marine waters highlighted by the increase of elements such as chlorides ( $\text{Cl}^-$ ) and sodium ( $\text{Na}^+$ ). This contribution could be due to fossil marine waters which are present in the deeper carbonate units as highlighted by Petrini et al. [66], and which outflows as natural thermal springs at Monfalcone (Italy), few kilometres southwest of the tapped point. Also other small water points, although in the nearby vicinity, have more

or less different physical-chemical characteristics. Being in a highly mature karst area, where over the time considerable fluctuations of the base level occurred, it is not possible to exclude, semi-independent articulated paths, activated only with considerable hydrostatic pressures.

**Author Contributions:** Conceptualization, C.C. and L.Z.; M.C.C., L.Z., K.M. and J.U.; Investigation, C.C.; Laboratory Sr analyses, F.F.S.; Data Analyses, C.C., K.M., F.F.S., L.Z.; Writing-Original Draft Preparation, C.C.; Writing-Review and Editing, C.C., K.M., L.Z. and J.U.; Supervision, L.Z.

**Funding:** This research was conducted in the framework of the Italy-Slovenia's cross-border cooperation program 2007–2013 during the 3-year project HYDROKARST (2012–2014) under the project contact number CB120. The Department of Mathematics and Geosciences (University of Trieste, Italy) was the Lead Partner, Project Partners were: Geological Survey of Slovenia, Karst Research Institute (Slovenia), AcegasApsAmgaGruppoHera (Italy), Kras water supply company Sežana (Slovenia), National Institute of Biology (Slovenia) and Direzione Centrale e ambiente, energia e politiche per la montagna della Regione Friuli Venezia Giulia (Italy).

**Acknowledgments:** The Authors would like to thank all the collaborators who helped in the sampling, data acquisition and elaboration phases as Philippe Turpaud, Francesco Treu, Enrico Zavagno, Chiara Boccali, Sara Biolchi, Fulvio Podda, Tamara Ferjan Stanič, Miroslav Medić and Franci Gabrovšek. The authors thanks the Park škocianke jame and the Società Adriatica di Speleologia for allowing the collection of the water samples in the caves. A particular thanks goes to Stefano Piselli and Daniela Sciolis who realized the chemical analyses on the water samples, to Paolo Sossi for his support on field and to Enrico Altran which coordinated the unit of the AcegasApsAmga. A special thanks goes to Barbara Stenni and to Marzia Michelini, who provided us with the precipitation isotopical data related to the rain gauge stations placed on the Italian side of the Classical Karst Region. An exceptional thanks goes to Franco Cucchi who had for first, several years ago, the idea of a cross-border ITA-SLO project and who, in the end won it giving to all of us the possibility to work together and obtain interesting results.

**Conflicts of Interest:** The authors declare no conflict of interest.

## References

- Zwahlen, F. *Vulnerability and Risk Mapping for the Protection of Carbonate (Karst) Aquifers*; European Commission: Brussels, Belgium, 2003.
- Barbieri, M.; Boschetti, T.; Petitta, M.; Tallini, M. Stable isotopes ( $^2\text{H}$ ,  $^{18}\text{O}$  and  $^{87}\text{Sr}/^{86}\text{Sr}$ ) and hydrochemistry monitoring for groundwater hydrodynamics analysis in a karst aquifer (Gran Sasso, central Italy). *Appl. Geochem.* **2005**, *20*, 2063–2081. [[CrossRef](#)]
- Wang, Y.; Cheng, H.; Edwards, R.L.; An, Z.; Wu, J.; Shen, C.; Dorale, J.A. A high-resolution absolute-dated late Pleistocene monsoon record from Hulu Cave, China. *Science* **2001**, *294*, 2345–2348. [[CrossRef](#)] [[PubMed](#)]
- Petelet-Giraud, E.; Negrel, Ph.; Casanova, J. Variability of  $^{87}\text{Sr}/^{86}\text{Sr}$  in water draining granite revealed after a double correction for atmospheric and anthropogenic inputs. *Hydrol. Sci. J.* **2003**, *48*, 729–742. [[CrossRef](#)]
- Han, G.; Liu, C.-Q. Water geochemistry controlled by carbonate dissolution: A study of the river waters draining karst-dominated terrain, Guizhou Province, China. *Chem. Geol.* **2004**, *204*, 1–21. [[CrossRef](#)]
- Doctor, D.; Calvin Alexander, E.; Petrič, M.; Kogovšek, J.; Urbanc, J.; Lojen, S.; Stichler, W. Quantification of karst aquifer discharge components during storm events through end-member mixing analysis using natural chemistry and stable isotopes as tracers. *Hydrogeol. J.* **2006**, *14*, 1171–1191. [[CrossRef](#)]
- Clark, I.D.; Fritz, P. *Environmental Isotopes in Hydrogeology*; CRC Press: Boca Raton, FL, USA, 1997; p. 352.
- Mook, W.G. *Introduction to Isotope Hydrology. Stable and Radioactive Isotopes of Hydrogen, Oxygen and Carbon*; Taylor & Francis Group: London, UK, 2006; p. 22.
- Johnson, T.M.; DePaolo, D.J. Reaction-transport models for radiocarbon in groundwater: The effects of longitudinal dispersion and the use of Sr isotope ratios to correct for water-rock interaction. *Water Resour. Res.* **1996**, *32*, 2203–2212. [[CrossRef](#)]
- Dogramaci, S.S. *Isotopes of Sulphur, Oxygen, Strontium and Carbon in Groundwater as Tracers of Mixing and Geochemical Processes, Murray Basin, Australia*. Ph.D. Thesis, University of Adelaide, Adelaide, Australia, 1998.
- De Villiers, S.; Compton, J.S.; Lavelle, M. The strontium isotope systematics of the Orange River, Southern Africa. *South Afr. J. Geol.* **1999**, *103*, 237–248. [[CrossRef](#)]
- Frost, C.D.; Toner, R.N. Strontium isotopic identification of water-rock interaction and ground water mixing. *Groundwater* **2004**, *42*, 418–432. [[CrossRef](#)]

13. Slejko, F.F.; Petrini, R.; Carulli, G.B.; Italiano, F.; Ditta, M. Preliminary geochemical and isotopic data on springs along the Fella-Sava fault zone (NE Italy). *Boll. Geofis. Teor. Appl.* **2007**, *48*, 423–434.
14. Ribeiro, S.; Azevedo, M.R.; Santos, J.F.; Medina, J.; Costa, A. Sr Isotopic Signatures of Portuguese Bottled Mineral Waters and Their Relationships with the Geological Setting. *Comunicações Geológicas*. **2014**, *101*, 29–37.
15. Jørgensen, N.; Banoeng-Yakubo, B.K. Environmental isotopes ( $^{18}\text{O}$ ,  $^2\text{H}$ , and  $^{87}\text{Sr}/^{86}\text{Sr}$ ) as a tool in groundwater investigations in the Keta Basin, Ghana. *Hydrogeol. J.* **2001**, *9*, 190–201.
16. Sappa, G.; Barbieri, M. Application of geochemical and isotopic analysis methods ( $^{87}\text{Sr}/^{86}\text{Sr}$ ) in hydrogeological characterization of some springs in Simbruini Mountains (Italy). In Proceedings of the International Symposium on Geology and Environment, Istanbul, Turkey, 2–6 September 1997; pp. 77–81.
17. Banner, J.L.; Musgrove, M.; Capo, R.C. Tracing ground-water evolution in a limestone aquifer using Sr isotopes: Effects of multiple sources of dissolved ions and mineral-solution reactions. *Geology* **1994**, *22*, 687–690. [[CrossRef](#)]
18. Boegan, E. Il Timavo: Studio sull'idrografia carsica subaerea e sotterranea. In *Memorie Del l'Istituto Italiano Di Speleologia*; Istituto Italiano Di Speleologia: Trieste, Italy, 1938; p. 251.
19. Mosetti, F.; D'Ambrosi, C. Alcune ricerche preliminari in merito a supposti legami di alimentazione fra il Timavo e l'Isonzo. *Boll. Geofis. Teor. Appl.* **1963**, *5*, 69–84.
20. Mosetti, F. Nuova interpretazione di un esperimento di marcatura radioattiva del Timavo. *Boll. Geofis. Teor. Appl.* **1965**, *7*, 218–243.
21. Gemiti, F.; Licciardello, M. Indagini sui rapporti di alimentazione delle acque del Carso triestino e goriziano mediante l'utilizzo di alcuni traccianti naturali. *Annali Gruppo Grotte Ass. 30 Ott.* **1977**, *6*, 43–61.
22. Cancian, G. *L'idrologia del Carso Goriziano-Triestino Tra L'Isonzo e Le Risorgive Del Timavo*; Museo Tridentino di Scienze Naturali: Trento, Italy, 1987.
23. Cucchi, F.; Forti, F. La "Cattura" del Timavo superiore a Vreme. Trieste: [s.n.]: Trieste, Italy, 1982.
24. Civita, M.; Cucchi, F.; Eusebio, A.; Garavoglia, S.; Maranzana, F.; Vigna, B. The Timavo hydrogeologic system: an important reservoir of supplementary water resources to be reclaimed and protected. *Acta Carsol.* **1995**, *24*, 169–186.
25. Cucchi, F.; Casagrande, G.; Manca, P.; Zini, L. Il Timavo ipogeo tra l'Abisso di Trebiciano e la Grotta Meravigliosa di Lazzaro Jerko. *Le Grotte d'Italia* **2001**, *2*, 39–48.
26. Samez, D.; Casagrande, G.; Cucchi, F.; Zini, L. *Idrodinamica dei Laghi di Doberdò e di Pietrarossa (Carso Classico, Italia): Relazioni con le Piene dei Fiumi Isonzo, Vipacco e Timavo*; Atti e Memorie della Commissione Grotte "E. Boegan": Trieste, Italy, 2005.
27. Kogovšek, J.; Petrič, M. Directions and dynamics of flow and transport of contaminants from the landfill near Sežana (SW Slovenia). *Acta Carsol.* **2007**, *36*, 413–424. [[CrossRef](#)]
28. Peric, B.; Gabrovšek, F.; Boschin, W.; Kogovšek, J.; Krafft, H. Karst water course tracing between ponor and springs: the Reka river example, Kras/Carso, SW Slovenia-NE Italy. In Proceedings of the International Conference on "Scientific Research in Show Caves, Postojna, Slovenia, 11–15 June 2014; pp. 32–33.
29. Zini, L.; Calligaris, C.; Zavagno, E. Classical Karst hydrodynamics: A sheared aquifer within Italy and Slovenia. *Proc. Int. Assoc. Hydrol. Sci.* **2014**, *364*, 499–504. [[CrossRef](#)]
30. Petrič, M.; Kogovšek, J. Identifying the characteristics of groundwater flow in the Classical Karst area (Slovenia/Italy) by means of tracer tests. *Environ. Earth Sci.* **2016**, *75*, 1446. [[CrossRef](#)]
31. Krivic, P.; Drobne, F.; Juren, A.; Kokol, L.; Strojjan, M.; Ravnikar, B. *Letno Poročilo 1986. Pitne, Tehnološke in Mineralne Vode. Hidrogeološke Raziskave Vodnih Virov v Karbonatnih Kamninah. Letno Poročilo Hidrogeološke Raziskave Zaledja Vodnih Virov pri Klaričih*; Report for Geological Survey of Slovenia; Geological Survey of Slovenia: Ljubljana, Slovenia, 1986; p. 96.
32. Pezdič, J.; Dolenc, T.; Krivic, P.; Urbanc, J. Environmental Isotope Studies Related to Groundwater Flow in the Central Slovenian Karst Region, Yugoslavia. In Proceedings of the 5th International Symposium on Underground Water Tracing, Athens, Greece, 22–27 September 1986; pp. 91–100.
33. Longinelli, A. Stable isotope hydrology of the classical Karst area. *Rend. Soc. Ital. Mineral. Petrol.* **1988**, *43*, 1175–1183.

34. Flora, O.; Longinelli, A. Stable isotope hydrology of classical karst area, Trieste, Italy. In Proceedings of the Isotope Techniques in the Study of the hydrology of fractured and fissured rocks, Panel Proceedings Series, Vienna, Austria, 17–21 November 1986; International Atomic Energy Agency (IAEA): Vienna, Austria, 1989; pp. 203–213.
35. Urbanc, J.; Kristan, S. Isotope investigation of the Brestovica water source during an intensive pumping test. *RMZ-Materials and Geoenvironment. Rud.-Met. Zb.* **1998**, *45*, 187–191.
36. Doctor, D.H.; Lojen, S.; Horvat, M. A stable isotope investigation of the Classical Karst aquifer: evaluating karst groundwater components for water quality preservation. *Acta Carsol.* **2000**, *29*, 79–82.
37. Doctor, D.H. Hydrologic connection and dynamics of water movement in the Classical Karst (Kras) aquifer: evidence from frequent chemical and stable isotope sampling. *Acta Carsol.* **2008**, *37*, 101–123. [[CrossRef](#)]
38. Cucchi, F.; Zini, L. Underground Timavo river monitoring (Classical Karst). *Acta Carsol.* **2002**, *31*, 75–84. [[CrossRef](#)]
39. Urbanc, J.; Mezga, K.; Zini, L. An assessment of capacity of Brestovica-Klariči karst water supply (Slovenia)/Ocena izdatnosti vodnega vira Brestovica-Klariči (Slovenija). *Acta Carsol.* **2012**, *41*, 89–100.
40. Buser, S. *Tolmač lista gorica. Osnovna Geološka Karta SFRJ*; Zvezni geološki zavod: Beograd, Serbia, 1973.
41. Cucchi, F.; Piano, C. *Carta Geologica del Carso Classico (Tratta Dalla Carta di Sintesi Geologica alla Scala 1:10000)*; Regione Autonoma Friuli Venezia Giulia, Direzione Centrale Ambiente, Energia e Politiche per la Montagna, Servizio Geologico: Trieste, Italy, 2013.
42. Jurkovšek, B.; Toman, M.; Ogorelec, B.; Šribar, L.; Drobne, K.; Poljak, M.; Šribar, L. *Formacijska Geološkakarta Južnega Dela Tržaško-komenske planote. Krednein Paleogenske Karbonatne Kammine/Geological Map of the Southern part of the Trieste-Komen Plateau (Slovenia), 1:50000*; Inštitut za Geologijo, Geotehniko Ingeofiziko: Ljubljana, Yugoslavia, 1996; p. 143.
43. Jurkovšek, B.; Biolchi, S.; Furlani, S.; Kolar-Jurkovšek, T.; Zini, L.; Jež, J.; Tunis, G.; Bavec, M.; Cucchi, F. Geology of the Classical Karst Region (SW Slovenia–NE Italy). *J. Maps* **2016**, *12*, 352–362. [[CrossRef](#)]
44. Calligaris, C.; Galli, M.; Gemiti, F.; Piselli, S.; Tentor, M.; Zini, L.; Cucchi, F. Electrical Conductivity as a tool to evaluate the various recharges of a Karst aquifer. In Proceedings of the 3th National Meeting on Hydrogeology, Cagliari, Italy, 14–16 June 2017; Università degli Studi di Cagliari: Cagliari, Italy, 2017.
45. Cucchi, F.; Zini, L.; Calligaris, C. *Le acque del Carso Classico, il Progetto Hydrokarst*; EUT: Trieste, Italy, 2015; p. 179.
46. Turpaud, P.; Zini, L.; Ravbar, N.; Cucchi, F.; Petric, M.; Urbanc, J. Development of a protocol for the karst water source protection zoning: Application to the Classical Karst Region (NE Italy and SW Slovenia). *Water Res. Manag.* **2018**, *32*, 1953–1968. [[CrossRef](#)]
47. Bensi, S.; Fanucci, F.; Podda, F. Strutture a macro e mesoscala delle Dinaridi triestine (Carta GEOCGT del FVG). *Rend. Online Soc. Geol. It.* **2009**, *5*, 32–35.
48. Zini, L.; Calligaris, C.; Forte, E.; Petronio, L.; Zavagno, E.; Boccali, C.; Cucchi, F. A multidisciplinary approach in sinkhole analysis: The Quinis village case study (NE-Italy). *Eng. Geol.* **2015**, *197*, 132–144. [[CrossRef](#)]
49. Zini, L.; Calligaris, C.; Cucchi, F. The challenge of tunneling through Mediterranean karst aquifers: The case study of Trieste (Italy). *Environ. Earth Sci.* **2015**, *74*, 281–295. [[CrossRef](#)]
50. Zini, L.; Casagrande, G.; Calligaris, C.; Cucchi, F.; Manca, P.; Treu, F.; Zavagno, E.; Biolchi, S. The Karst hydrostructure of the Mount Canin (Julian Alps, Italy and Slovenia). In *Hydrogeological and Environment. Investigations in Karst System*; Springer Nature Switzerland AG: Basel, Switzerland, 2014; pp. 219–226.
51. Calligaris, C.; Boschin, W.; Cucchi, F.; Zini, L. The karst hydrostructure of the Verzegnis group (NE Italy). *Carbonate Evaporite* **2016**, *31*, 407–420. [[CrossRef](#)]
52. Calligaris, C.; Devoto, S.; Zini, L.; Cucchi, F. An integrated approach for investigations of ground-subsidence phenomena in the Ovaro village (NE Italy). In *EuroKarst 2016, Neuchâtel*; Springer: Neuchâtel, Germany, 2017; pp. 71–77.
53. Cvijić, J. Das Karstphänomenon. Versuch einer morphologischen Monographie. *Geogr. Abh. Wien* **1893**, *5*, 218–329.
54. Ford, D. Jovan Cvijić and the founding of karst geomorphology. *Environ. Geol.* **2007**, *51*, 675–684. [[CrossRef](#)]
55. Galli, M. *Timavo: Esplorazione e Studi*; EUT Edizioni Università di Trieste: Trieste, Italy, 1999; p. 195.
56. Zini, L.; Calligaris, C.; Treu, F. *Risorse Idriche Sotterranee Del Friuli Venezia Giulia: Sostenibilità del L'attuale Utilizzo*; EUT Edizioni Università di Trieste: Trieste, Italy, 2011; p. 88.

57. Timeus, G. Nei misteri del mondo sotterraneo-Risultati delle ricerche idrologiche sul Timavo 1895–1914, 1918–1927. *Alpi Giulie* **1928**, *29*, 1–39.
58. Gemiti, F. La portata del Timavo alle risorgive di S. Giovanni di Duino. *Annali Gruppo Grotte Ass. 30 Ott.* **1984**, *7*, 23–41.
59. Gemiti, F. Portata liquida e portata solida del Timavo alle risorgive di S. Giovanni di Duino. *Hydrores* **1995**, *13*, 75–88.
60. Mosetti, F.; Eriksson, E. Misura della velocità di deflusso di un corso d'acqua sotterraneo mediante esame del comportamento dell'oscillazione annua della temperatura dell'acqua. *Boll. Geofis. Teor. Appl.* **1964**, *6*, 68–73.
61. Gabrovšek, F.; Borut, P. Monitoring the flood pulses in the epiphreatic zone of karst aquifers: The case of Reka river system, Karst plateau, SW Slovenia. *Acta Carsol.* **2006**, *35*, 35–45. [[CrossRef](#)]
62. Gemiti, F. Indagini idrochimiche alle risorgive del Timavo. Atti e Mem. Comm. Grotte E. Boegan **1994**, *31*, 73–83.
63. Wheeler, M.D.; Newman, S.M.; Orr-Ewing, A.J.; Ashfold, M.N. Cavity ring-down spectroscopy. *J. Chem. Soc. Faraday Trans.* **1998**, *94*, 337–351. [[CrossRef](#)]
64. Hut, G. *Consultants' Group Meeting on Stable Isotope Reference Samples for Geochemical and Hydrological Investigations*; International Atomic Energy Agency: Vienna, Austria, 1987; p. 42.
65. Ludwig, K.R. *Analyst. A Computer Program for Control of a Thermal Ionization Single-Collector Mass Spectrometer*; USGS Open-file report: Leston, VA, USA, 1994.
66. Petrini, R.; Italiano, F.; Ponton, M.; Slejko, F.F.; Aviani, U.; Zini, L. Geochemistry and isotope geochemistry of the Monfalcone thermal waters (northern Italy): Inference on the deep geothermal reservoir. *Hydrogeol. J.* **2013**, *21*, 1275–1287. [[CrossRef](#)]
67. Craig, H. Isotopic variations in meteoric waters. *Science* **1961**, *133*, 1702–1703. [[CrossRef](#)] [[PubMed](#)]
68. Longinelli, A.; Selmo, E. Isotopic composition of precipitation in Italy: A first overall map. *J. Hydrol.* **2003**, *270*, 75–88.
69. Vreča, P.; Bronić, I.K.; Horvatinčić, N.; Barešić, J. Isotopic characteristics of precipitation in Slovenia and Croatia: Comparison of continental and maritime stations. *J. Hydrol.* **2006**, *330*, 457–469. [[CrossRef](#)]
70. Vreča, P.; Bronić, I.K.; Leis, A. Isotopic composition of precipitation in Portorož (Slovenia). *Geologija* **2011**, *54*, 129–138.
71. Gat, J.R.; Carmi, H. Evolution of the isotopic composition of atmospheric waters in the Mediterranean Sea Area. *J. Geophys. Res.* **1970**, *75*, 3039–3040. [[CrossRef](#)]
72. Sappa, G.; Barbieri, M.; Ergul, S.; Ferranti, F. Hydrogeological conceptual model of groundwater from carbonate aquifers using environmental isotopes ( $^{18}\text{O}$ ,  $^2\text{H}$ ) and chemical tracers: A case study in southern Latium Region, Central Italy. *J. Water Resour. Prot.* **2012**, *4*, 695–716. [[CrossRef](#)]
73. Gat, J.R.; Dansgaard, W. Stable isotope survey of the freshwater occurrences in Israel and the Jordon Rift Valley. *J. Hydrol.* **1972**, *16*, 177–211. [[CrossRef](#)]
74. Cruz-San Julian, J.; Araguas, L.; Rozanski, K.; Benavente, J.; Cardenal, J.; Hidalgo, M.C.; Garcia-Lopez, S.; Martinez-Garrido, J.C.; Moral, F.; Olias, M. Sources of precipitation over south-eastern Spain and groundwater recharge. An isotopic study. *Tellus* **1992**, *44*, 226–236. [[CrossRef](#)]
75. Rozanski, K.; Araguas-Araguas, L.; Gonfiantini, R. Isotope patterns in modern global precipitation. In *Climate Change in Continental Isotope Records*; American Geophysical Union: Washington, DC, USA, 1993; pp. 1–35.
76. Fröhlich, K.; Gibson, J.J.; Aggarwal, P.K. Deuterium excess in precipitation and its climatological significance. In *Proceedings of the International Conference on Study of Environmental Change Using Isotope Techniques*, Vienna, Austria, 23–27 April 2001; International Atomic Energy Agency: Vienna, Austria, 2002.
77. Ingraham, N.L. *Systematics of isotopic variations in precipitation. Isotope Tracers in Catchment Hydrology*; Elsevier: Amsterdam, The Netherlands, 1993; pp. 87–118.
78. Michellini, M. *Studio Geochimico Isotopico Delle Precipitazioni del Friuli Venezia Giulia*. Ph.D. Thesis, Università degli Studi di Trieste, Trieste, Italy, 2012.
79. Mezga, K.; Urbanc, J.; Cerar, S. The isotope altitude effect reflected in groundwater: a case study from Slovenia. *Isot. Environ. Health Stud.* **2014**, *50*, 33–51. [[CrossRef](#)] [[PubMed](#)]
80. Roller-Lutz, Z.; Mance, D.; Hunjak, T.; Lutz, H.O. On the isotopic altitude effect of precipitation in the Northern Adriatic (Croatia). In *Isotopes in Hydrology, Marine Ecosystems and Climate Change Studies, Proceedings of an International Symposium, Monaco, Germany, 27 March–1 April 2011*; International Atomic Energy Agency: Vienna, Austria, 2013; pp. 99–105.



81. Horton, T.W.; Defliese, W.F.; Tripathi, A.K.; Oze, C. Evaporation induced  $^{18}\text{O}$  and  $^{13}\text{C}$  enrichment in lake systems: A global perspective on hydrologic balance effects. *Quat. Sci. Rev.* **2016**, *131*, 365–379. [[CrossRef](#)]
82. Palmer, M.R.; Edmond, J.M. Controls over the strontium isotope composition of river water. *Geochim. Cosmochim. Acta* **1992**, *56*, 2099–2111. [[CrossRef](#)]
83. Johnson, T.M.; De Paolo, D.J. Interpretation of isotopic data in groundwater-rock systems: model development and application to Sr isotope data from Yucca Mountain. *Water Resour. Res.* **1994**, *30*, 1571–1587. [[CrossRef](#)]
84. Katz, B.G.; Bullen, T.D. The combined use of  $^{87}\text{Sr}/^{86}\text{Sr}$  and carbon and water isotopes to study the hydrochemical interaction between groundwater and lake water in mantled karst. *Geochim. Cosmochim. Acta* **1996**, *60*, 5075–5087. [[CrossRef](#)]
85. Oetting, G.C.; Banner, J.L.; Sharp, J.M., Jr. Regional controls on the geochemical evolution of saline groundwaters in the Edwards aquifer, central Texas. *J. Hydrol.* **1996**, *181*, 251–283. [[CrossRef](#)]
86. Gosselin, D.C.; Nabelek, P.E.; Peterman, Z.E.; Sibray, S. A reconnaissance study of oxygen, hydrogen and strontium isotopes in geochemically diverse lakes, Western Nebraska, USA. *J. Paleolimnol.* **1997**, *17*, 51–65. [[CrossRef](#)]
87. Armstrong, S.C.; Sturchio, N.C. Strontium isotopic evidence on the chemical evolution of pore waters in the Milk River Aquifer, Alberta, Canada. *Appl. Geochem.* **1998**, *13*, 463–475. [[CrossRef](#)]
88. Johnson, T.M.; Roback, R.C.; McLing, T.L.; Bullen, T.D.; De Paolo, D.J.; Doughty, C.; Hunt, R.J.; Smith, R.W.; DeWayne Cecil, L.; Murrell, M.T. Groundwater “fast paths” in the Snake River Plain aquifer: Radiogenic isotope ratios as natural groundwater tracers. *Geology* **2000**, *28*, 871–874. [[CrossRef](#)]
89. Gosselin, D.C.; Harvey, F.E.; Frost, C.; Stotler, R.; Macfarlane, P.A. Strontium isotope geochemistry of groundwater in the central part of the Dakota (Great Plains) aquifer, USA. *Appl. Geochem.* **2004**, *19*, 359–377. [[CrossRef](#)]
90. Musgrove, M.; Banner, J.L. Controls on the spatial and temporal variability of vadose dripwater geochemistry: Edwards Aquifer, central Texas. *Geochim. Cosmochim. Acta* **2004**, *68*, 1007–1020. [[CrossRef](#)]
91. Musgrove, M.; Stern, L.A.; Banner, J.L. Springwater geochemistry at Honey Creek State Natural Area, central Texas: Implications for surface water and groundwater interaction in a karst aquifer. *J. Hydrol.* **2010**, *388*, 144–156. [[CrossRef](#)]
92. Négrel, P.; Petelet-Giraud, E. Strontium isotopes as tracers of groundwater-induced floods: The Somme case study (France). *J. Hydrol.* **2004**, *305*, 99–119. [[CrossRef](#)]
93. Valentinuz, F. Caratterizzazione Geochimica Dell’acquifero del Carso Classico. Bachelor’s Thesis, Università degli Studi di Trieste, Trieste, Italy, 2010.
94. Neumann, K.; Dreiss, S. Strontium  $^{87}\text{Sr}/^{86}\text{Sr}$  ratios as tracers in groundwater and surface waters in Mono Basin, California. *Water Resour. Res.* **1995**, *31*, 3183–3193. [[CrossRef](#)]
95. Hogan, J.F.; Blum, J.D.; Siegel, D.I.; Glaser, P.H.  $^{87}\text{Sr}/^{86}\text{Sr}$  as a tracer of groundwater discharge and precipitation recharge in the Glacial Lake Agassiz Peatlands, northern Minnesota. *Water Resour. Res.* **2000**, *36*, 3701–3710. [[CrossRef](#)]
96. Negrel, P.; Petelet-Giraud, E.; Widory, D. Strontium isotope geochemistry of alluvial groundwater: a tracer for groundwater resources characterization. *Hydrol. Earth Syst. Sci. Discuss.* **2004**, *8*, 959–972. [[CrossRef](#)]

